**Noname manuscript No.**
(will be inserted by the editor)

# Timed Abstractions for Distributed Cooperative Manipulation

**Christos K. Verginis** · **Dimos V. Dimarogonas**

Received: date / Accepted: date

**Abstract** This paper addresses the problem of deriving well-defined timed abstractions for the decentralized cooperative manipulation of a single object by $N$ robotic agents. In particular, we propose a distributed model-free control protocol for the trajectory tracking of the cooperatively manipulated object without necessitating feedback of the contact forces/torques or inter-agent communication. Certain pre-specified performance functions determine the transient and steady state of the coupled object-agents system. The latter, along with a region partition of the workspace that depends on the physical volume of the object and the agents, allows us to define timed transitions for the coupled system among the derived workspace regions. Therefore, we abstract its motion as a finite transition system and, by employing standard automata-based methodologies, we define high level complex tasks for the object that can be encoded by timed temporal logics. In addition, we use load sharing coefficients to represent potential differences in power capabilities among the agents. Finally, realistic simulation studies verify the validity of the proposed scheme.

**Keywords** Timed abstractions · Cooperative Manipulation · Formal verification · Robotics · Multi-agent systems · Robust control.

This work was supported by funding from the Knut and Alice Wallenberg Foundation, the Swedish Research Council (VR), the European Union's Horizon 2020 Research and Innovation Programme under the Grant Agreement No. 644128 (AEROWORKS), the H2020 ERC Starting Grant BUCOPHSYS and the EU H2020 Research and Innovation Programme under GA No. 731869 (Co4Robots).

C. K. Verginis (✉) · Dimos V. Dimarogonas
KTH Royal Institute of Technology, Osquldas Väg 10, 100 44 Stockholm, Sweden
Tel.: +46-70-4438285
E-mail: cverginis@kth.se

D. V. Dimarogonas
E-mail: dimos@kth.se

## 1 Introduction

Multi-agent systems have gained significant attention over the last decades, since they provide several advantages with respect to single-agent setups. In the case of object manipulation, complex tasks involving heavy/large payloads and difficult maneuvers necessitate the employment of more than one robot. The problem of cooperative manipulation control has been studied extensively, using centralized schemes, where a central computer handles the agents' behavior, as well as decentralized setups, where each agent determines its actions on its own, either with partial or no communication at all (Liu and Arimoto, 1998; Caccavale et al., 2008; Heck et al., 2013; Szewczyk et al., 2002; Tsiamis et al., 2015b; Petitti et al., 2016; Wang and Schwager, 2016; Sugar and Kumar, 2002; Tanner et al., 2003; Erhart and Hirche, 2013; Markdahl et al., 2012).

In contrast to the related literature, which mainly considers the trajectory tracking of the manipulated object, we are here interested in complex tasks over time, such as "never take the object to dangerous regions" or "keep moving the object from region A to B within a predefined time interval" which must be executed via the control actions of the agents. Such tasks can be expressed by temporal logic languages, which can describe complex planning objectives more efficiently than the well-studied navigation algorithms. Linear Temporal Logic (LTL) is the most common language that has been incorporated in the multi-agent motion planning problem (Guo et al., 2014; Chen et al., 2012; Zhang and Cowlagi, 2016; Filippidis and Murray, 2016; Diaz-Mercado et al., 2015), without however considering time specifications. Metric and Metric Interval Temporal Logic (MTL, MITL) (Alur et al., 1996; Souza and Prabhakar, 2007; Alur and Dill, 1994), as well as Time Window Temporal Logic (TWTL) are languages that encode time specifications and

were used for multi-agent motion planning in (Nikou et al., 2016; Karaman and Frazzoli, 2011; Aksaray et al., 2016).

In order to be able to define temporal logic objectives, the continuous-time system must be abstracted to a higher-level discrete representation that incorporates the motion and the actions of the system. Discrete abstractions of continuous-time systems have been considered in a variety of works, including (Zamani et al., 2014; Belta and Kumar, 2004; Belta and Habets, 2006; Adzkiya et al., 2013; Kloetzer and Belta, 2008; Rungger et al., 2015; Boskos and Dimarogonas, 2015; Tiwari, 2008; Reissig, 2011). In this work, however, we are interested in defining timed abstractions for a system that consists of $N$ robotic agents (mobile bases with robotic manipulators) rigidly grasping an object.

Regarding robotic manipulation, high level planning techniques have been proposed in (Yamashita et al., 2003; Cheng et al., 2009; Lionis and Kyriakopoulos, 2005) using common planning methods like potential fields in the configuration space and $A^*$ algorithms. In (Lionis and Kyriakopoulos, 2005) the motion planning problem for a group of unicycles manipulating a rigid body is addressed and in (Cheng et al., 2009) an abstraction methodology is introduced; LTL specifications are employed in (Tsiamis et al., 2015a), where two mobile robots transport an object in a leader-follower scheme. Additionally, temporal logic formulas are utilized in (Muthusamy and Kyrki, 2014) for dexterous manipulation through robotic fingers and in (He et al., 2015) for single manipulation tasks, without, however, incorporating the dynamics of the robotic arm in the abstracted model. A hybrid framework for cooperative manipulation is presented in (Chaimowicz et al., 2003).

For the continuous control part, impedance and/or force control is the most common methodology (Caccavale et al., 2008; Heck et al., 2013; Szewczyk et al., 2002; Tsiamis et al., 2015b; Parra-Vega et al., 2013), in which the robotic arms employ sensors to obtain feedback of the contact forces which, however, may result to performance decline due to sensor noise or mounting difficulties; (Michael et al., 2011) considers the optimization-based load transportation by multiple quadrotors using cables and (Wang and Schwager, 2016; Stroupe et al., 2005) consider kinematic-based approaches. Moreover, most works in the related literature consider known dynamic models and/or parameters of the object and the agents, whose accurate knowledge, however, can be a challenging issue. Object parameter estimation in cooperative manipulation schemes has been considered in (Franchi et al., 2014, 2015) and a reinforcement learning approach has been adopted in (Palunko et al., 2014).

In this paper, we study the timed abstraction of a system comprising of $N$ robotic agents rigidly grasping an object. In particular, we develop a distributed model-free control protocol for the trajectory tracking of the cooperatively manipulated object with prescribed transient and steady state performance, which allows us to model the motion of the coupled object-agents system as a finite transition system. Then, by employing formal verification-based methodologies, we derive a path that satisfies a given MITL task. The control scheme does not use any force/torque information at the contact points or any inter-agent communication and incorporates load sharing coefficients to account for differences in power capabilities among the agents.

This paper extends our previous work (Verginis and Dimarogonas, 2016) in the following directions: firstly, we express the dynamic models of the object and the agents by employing angular velocities and accelerations for the agents' end-effector and the object's center of mass (contrary to Euler angle accelerations used in (Verginis and Dimarogonas, 2016)). This is more accurate for real-time scenarios and also introduces the realistic problem of representation singularities for the object's center of mass, which is resolved by our control methodology. Secondly, we perform simulations in the environment of V-REP (Rohmer et al., 2013), which constitutes a realistic physics simulator, and we verify thus the robustness of the proposed control scheme.

The rest of the paper is organized as follows: Section 2 introduces notation and preliminary background. Section 3 describes the problem formulation and the overall system's model. The control strategy is presented in Section 4. Section 5 verifies our approach through simulation results and Section 6 concludes the paper.

## 2 Notation and Preliminaries

### 2.1 Notation

The set of positive integers is denoted as $\mathbb{N}$ and the real $n$-coordinate space, with $n \in \mathbb{N}$, as $\mathbb{R}^n$; $\mathbb{R}^n_{\geq 0}$ and $\mathbb{R}^n_{>0}$ are the sets of real $n$-vectors with all elements nonnegative and positive, respectively. Given a set $S$, $2^S$ is the set of all subsets of $S$ and, given a finite sequence $s_1,\dots,s_n$ of elements in $S$, with $n \in \mathbb{N}$, we denote by $(s_1,\dots,s_n)^\omega$ the infinite sequence $s_1,\dots,s_n,s_1,\dots,s_n,s_1,\dots$ created by repeating $s_1,\dots,s_n$. The minimum eigenvalue of a matrix $A \in \mathbb{R}^{n\times n}, n \in \mathbb{N}$, is denoted as $\lambda_{\min}(A)$. Moreover, $\|x\|$ is the Euclidean norm of a vector $x \in \mathbb{R}^n$. The $n \times n$ identity matrix and the $n \times m$ matrix with zero entries are denoted as $I_n$ and $0_{n\times m}$, respectively, with $n,m \in \mathbb{N}$. The values of a Boolean variable are $\top$ (True) and $\bot$ (False). The vector connecting the origins of coordinate frames $\{A\}$ and $\{B\}$ expressed in frame $\{C\}$ coordinates in 3-D space is denoted as $p^C_{B/A} \in \mathbb{R}^3$. Given $a \in \mathbb{R}^3, S(a)$ is the skew-symmetric matrix defined according to $S(a)b = a \times b$, where $\times$ is the cross product operator. We further denote as $\eta_{A/B} = [\phi_{A/B}, \theta_{A/B}, \psi_{A/B}]^T \in \mathbb{T}^3 \subset \mathbb{R}^3$ the $x$-$y$-$z$ Euler angles representing the orientation of frame $\{A\}$ with respect to frame $\{B\}$, with $\phi_{A/B}, \theta_{A/B} \in [-\pi, \pi]$ and $\theta_{A/B} \in [-\frac{\pi}{2}, \frac{\pi}{2}]$,

where $\mathbb{T}^3$ is the 3-D torus; Moreover, $R_A^B \in SO(3)$ is the rotation matrix associated with the same orientation and $SO(3)$ is the 3-D rotation group. The angular velocity of frame $\{B\}$ with respect to $\{A\}$, expressed in frame $\{C\}$ coordinates, is denoted as $\omega_{B/A}^C \in \mathbb{R}^3$ and it holds that $\dot{R}_A^B = S(\omega_{B/A}^A)R_A^B$; $\mathcal{B}(c,r)$ denotes the 3-D sphere of radius $r \geq 0$ and center $c \in \mathbb{R}^3$ and $d : \mathbb{R}^3 \times \mathbb{R}^3 \to \mathbb{R}_{\geq 0}$ is the 3-D Euclidean distance. We further define the set $\mathbb{M} = \mathbb{R}^3 \times \mathbb{T}^3$ as well as $\mathcal{N} = \{1,\ldots,N\}$. For notational brevity, when a coordinate frame corresponds to an inertial frame of reference $\{I\}$, we will omit its explicit notation (e.g., $p_B = p_{B/I}^I, \omega_B = \omega_{B/I}^I, R_A = R_A^I$, etc.). Finally, all vector and matrix differentiations will be with respect to an inertial frame $\{I\}$, unless otherwise stated.

## 2.2 Metric Interval Temporal Logic (MITL)

**Definition 1** (Alur and Dill, 1994) The time sequence $t_1 t_2 \ldots$ is an infinite sequence of time values $t_j \in \mathbb{R}_{\geq 0}, \forall j \in \mathbb{N}$, satisfying the following constraints:

- Monotonicity: $t_j < t_{j+1}, \forall j \in \mathbb{N}$.
- Progress: $\forall t' \in \mathbb{R}_{\geq 0}, \exists j \geq 1$ such that $t_j \geq t'$.

An *atomic proposition* $\mathcal{P}$ is a statement over the problem variables and parameters that is either True ($\top$) of False ($\bot$) at a given time instance.

**Definition 2** Let $\mathcal{AP}$ be a finite set of atomic propositions. A timed word $w$ over $\mathcal{AP}$ is an infinite sequence $w = (w_1,t_1)(w_2,t_2),\ldots$, where $w_1 w_2 \ldots$ is an infinite word over $2^{\mathcal{AP}}$ and $t_1 t_2 \ldots$ is a time sequence according to Definition 1.

**Definition 3** A *Weighted Transition System (WTS)* is a tuple

$$(S, S_0, \xrightarrow{\mathcal{T}}, \mathcal{AP}, \mathcal{L}, \gamma), \tag{1}$$

where

- $S$ is a finite set of states,
- $S_0 \subseteq S$ is a set of initial states,
- $\xrightarrow{\mathcal{T}} \subseteq S \times S$ is a transition relation,
- $\mathcal{AP}$ is a finite set of atomic propositions,
- $\mathcal{L} : S \to 2^{\mathcal{AP}}$ is a labeling function and
- $\gamma : (\xrightarrow{\mathcal{T}}) \to \mathbb{R}_{\geq 0}$ is a map that assigns a positive weight to each transition.

**Definition 4** A *timed run* of a WTS is an infinite sequence $r = (r_1,t_1)(r_2,t_2)\ldots$ such that $r_1 \in S_0$, and $r_j \in S, (r_j, r_{j+1}) \in \xrightarrow{\mathcal{T}}, \forall j \in \mathbb{N}$. The time stamps $t_j$ are inductively defined as

1. $t_1 = 0$,
2. $t_{j+1} = t_j + \gamma(r_j, r_{j+1}), \forall j \in \mathbb{N}$.

The timed run $r$ generates a timed word $w(r) = w_1(r_1)w_2(r_2)\cdots = (\mathcal{L}(r_1),t_1)(\mathcal{L}(r_2),t_2)\ldots$ over the set $2^{\mathcal{AP}}$, where $\mathcal{L}(r_j)$ is the subset of atomic propositions that are true at state $r_j$ at time $t_j, \forall j \in \mathbb{N}$.

The syntax of *Metric Interval Temporal Logic (MITL)* over a set of atomic propositions $\mathcal{AP}$ is defined by the grammar

$$\phi := p \,|\, \neg\phi \,|\, \phi_1 \wedge \phi_2 |\, \bigcirc_I \phi \,|\, \Diamond_I \phi \,|\, \Box_I \phi \,|\, \phi_1 \mathcal{U}_I \phi_2, \tag{2}$$

where $p \in \mathcal{AP}$, and $\bigcirc, \Diamond, \Box$ and $\mathcal{U}$ are the next, future, always and until operators, respectively; $I$ is a nonempty time interval in one of the following forms: $[i_1,i_2], [i_1,i_2), (i_1,i_2], (i_1,i_2), [i_1,\infty), (i_1,\infty)$ with $i_1, i_2 \in \mathbb{R}_{\geq 0}, i_2 > i_1$. MITL can be interpreted either in continuous or point-wise semantics. We utilize the latter and interpret MITL formulas over timed runs such as the ones produced by a WTS.

**Definition 5** (Souza and Prabhakar, 2007; Ouaknine and Worrell, 2005) Given a run $r = (r_1,t_1)(r_2,t_2)\ldots$ of a WTS and a MITL formula $\phi$, we define $(r,j) \models \phi, j \in \mathbb{N}$ ($r$ satisfies $\phi$ at $j$) as follows:

$$\begin{aligned}
&(r,j) \models p \Leftrightarrow p \in \mathcal{L}(r_j),\\
&(r,j) \models \neg\phi \Leftrightarrow (r,j) \not\models \phi\\
&(r,j) \models \phi_1 \wedge \phi_2 \Leftrightarrow (r,j) \models \phi_1 \text{ and } (r,j) \models \phi_2\\
&(r,j) \models \bigcirc_I \phi \Leftrightarrow (r,j+1) \models \phi \text{ and } t_{j+1} - t_j \in I\\
&(r,j) \models \phi_1 \mathcal{U}_I \phi_2 \Leftrightarrow \exists k, j, \text{with} j \leq k, \text{s.t. } (r,k) \models \phi_2, t_k - t_j \in I\\
&\qquad \text{and } (r,m) \models \phi_1, \forall m \in \{j,\ldots,k\}
\end{aligned}$$

Also, $\Diamond_I \phi = \top \mathcal{U}_I \phi$ and $\Box_I \phi = \neg\Diamond_I \neg\phi$. The sequence $r$ satisfies $\phi$, denoted as $r \models \phi$, if and only if $(r,1) \models \phi$.

## 2.3 Prescribed Performance

Prescribed Performance control, recently proposed in (Bechlioulis and Rovithakis, 2014), describes the behavior where a tracking error $e(t) : \mathbb{R}_{\geq 0} \to \mathbb{R}$ evolves strictly within a predefined region that is bounded by certain functions of time, achieving prescribed transient and steady state perfromance. The mathematical expression of prescribed performance is given by the following inequalities:

$$-\rho_L(t) < e(t) < \rho_U(t), \;\; \forall t \in \mathbb{R}_{\geq 0}, \tag{3}$$

where $\rho_L(t), \rho_U(t)$ are smooth and bounded decaying functions of time satisfying $\lim_{t\to\infty} \rho_L(t) > 0$ and $\lim_{t\to\infty} \rho_U(t) > 0$, called performance functions. We focus on the case of the exponential performance functions $\rho_i(t) = (\rho_i^0 - \rho_i^\infty)e^{-l_i t} + \rho_i^\infty$, with $\rho_i^0, \rho_i^\infty, l_i \in \mathbb{R}_{>0}, i \in \{U,L\}$, appropriately chosen constants. More specifically, the constants $\rho_L^0 = \rho_L(0), \rho_U^0 = \rho_U(0)$ are selected such that $\rho_U^0 > e(0) > \rho_L^0$ and the constants $\rho_L^\infty = \lim_{t\to\infty} \rho_L(t), \rho_U^\infty = \lim_{t\to\infty} \rho_U(t)$ represent the maximum allowable size of the tracking error $e(t)$ at steady state, which may be set arbitrarily small to a value reflecting the resolution of the measurement device, thus achieving practical convergence of $e(t)$ to zero. Moreover, the decreasing

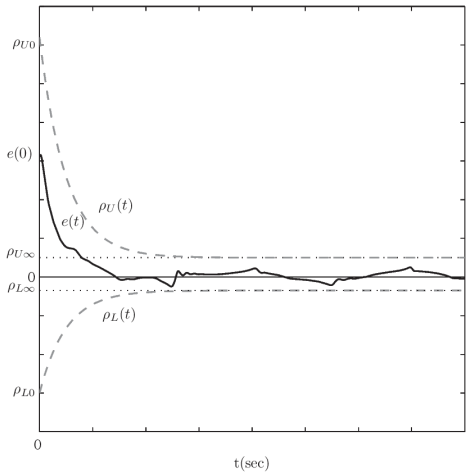


**Fig. 1** Graphical illustration of the prescribed performance definition

rate of $\rho_L(t), \rho_U(t)$, which is affected by the constants $l_L, l_U$ in this case, introduces a lower bound on the required speed of convergence of $e(t)$. Therefore, the approriate selection of the performance functions $\rho_L(t), \rho_U(t)$ imposes performance characteristics on the tracking error $e(t)$.

### 2.4 Dynamical Systems

Consider the initial value problem:

$$\dot{\xi} = H(t,\xi),\ \xi(t_0) = \xi^0 \in \Omega_\xi, \tag{4}$$

with $H : [t_0, +\infty) \times \Omega_\xi \to \mathbb{R}^n$ where $\Omega_\xi \subset \mathbb{R}^n$ is a non-empty open set.

**Definition 6** (Sontag, 2013) A solution $\xi(t)$ of the initial value problem (4) is maximal if it has no proper right extension that is also a solution of (4).

**Theorem 1** *(Sontag, 2013) Consider the initial value problem* (4)*. Assume that $H(t,\xi)$ is: a) locally Lipschitz on $\xi$ for almost all $t \in [t_0, +\infty)$, b) piecewise continuous on $t$ for each fixed $\xi \in \Omega_\xi$ and c) locally integrable on $t$ for each fixed $\xi \in \Omega_\xi$. Then, there exists a maximal solution $\xi(t)$ of* (4) *on $[t_0, \tau_{\max})$, with $\tau_{\max} > t_0$, such that $\xi(t) \in \Omega_\xi, \forall t \in [t_0, \tau_{\max})$.*

**Proposition 1** *(Sontag, 2013) Assume that the hypotheses of Theorem 1 hold. For a maximal solution $\xi(t)$ on the time interval $[t_0, \tau_{\max})$, with $\tau_{\max} < \infty$, and for any compact set $\Omega'_\xi \subset \Omega_\xi$ there exists a time instant $t' \in [t_0, \tau_{\max})$ such that $\xi(t') \notin \Omega'_\xi$.*

## 3 Problem Formulation

Consider a bounded workspace $\mathcal{W} \subset \mathbb{R}^3$ containing $N$ robotic agents rigidly grasping an object, as shown in Fig. 2. The agents are considered to be fully actuated and they consist

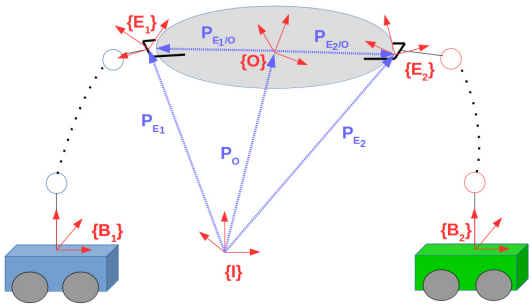


**Fig. 2** Two robotic arms rigidly grasping an object.

of a base that is able to move around the workspace (e.g., mobile or aerial vehicle) and a robotic arm. The reference frames corresponding to the $i$-th end-effector and the object's center of mass are denoted with $\{E_i\}$ and $\{O\}$, respectively, whereas $\{I\}$ corresponds to an inertial reference frame. The rigidity of the grasps implies that the agents can exert any force/torque along every direction to the object. We consider that each agent $i$ knows only its own state, position and velocity, as well as its own and the object's geometric parameters. More specifically, we assume that each agent $i$ knows the distance from its grasping point $\{E_i\}$ to the object's center of mass $\{O\}$ as well as the relative orientation offset between the two frames $\{E_i\}$ and $\{O\}$. This information can be either retrieved on-line via appropriate sensors or transmitted off-line to the agents, without the need of inter-agent on-line communication. Finally, no interaction force/torque measurements are required and the dynamic model of the object and the agents is considered unknown.

### 3.1 System model

#### *3.1.1* ***Robotic agents***

We denote by $q_i \in \mathbb{R}^{n_i}$ the joint space variables of agent $i \in \mathcal{N}$, with $n_i = n_{\alpha_i} + 6$, $q_i = [p_{B_i}^T, \eta_{B_i}^T, \alpha_i^T]^T$, where $p_{B_i} \in \mathbb{R}^3, \eta_{B_i} = [\phi_{B_i}, \theta_{B_i}, \psi_{B_i}]^T \in \mathbb{T}^3 \subset \mathbb{R}^3$ is the position and Euler-angle orientation of the agent's base, and $\alpha_i = [\alpha_{i_1}, \ldots, \alpha_{i_{n_i}}]^T \in \mathbb{R}^{n_{\alpha_i}}, n_{\alpha_i} > 0$, are the degrees of freedom of the robotic arm. The overall joint space configuration vector is denoted as $q = [q_1^T, \ldots, q_N^T]^T \in \mathbb{R}^n$, with $n = \sum_{i\in\mathcal{N}} n_i$. In addition, we denote as $p_{E_i} \in \mathbb{R}^3, \eta_{E_i} \in \mathbb{T}^3$ the position and Euler-angle orientation of agent $i$'s end-effector, and $x_{E_i} = [p_{E_i}^T, \eta_{E_i}^T]^T, i \in \mathcal{N}$. Let also $v_i \in \mathbb{R}^6$ denote the velocity of agent $i$'s end-effector, with $v_i = [\dot{p}_{E_i}^T, \omega_{E_i}^T]^T$, whereas $\dot{p}_{B_i}, \omega_{B_i} \in \mathbb{R}^3$ is the linear and angular velocity of the agent's base.

We consider that each agent $i \in \mathcal{N}$ has access to its own state $q_i$ as well as $\dot{p}_{B_i}^{B_i}, \omega_{B_i}^{B_i}$, and $\dot{\alpha}_i$ via on-board sensors. Then, $\dot{p}_{B_i}, \omega_{B_i}$ can be obtained via $\dot{p}_{B_i} = R_{B_i}(\eta_{B_i})\dot{p}_{B_i}^{B_i}$, $\omega_{B_i} = R_{B_i}(\eta_{B_i})\omega_{B_i}^{B_i}$, where $R_{B_i} : \mathbb{T}^3 \to SO(3)$ is the rotation matrix of the agent $i$'s base. Moreover, $\dot{\eta}_{B_i}$ is related to $\omega_{B_i}$ via

$\omega_{B_i} = J_{B_i}(\eta_{B_i})\dot{\eta}_{B_i}$, where $J_{B_i} : \mathbb{T}^3 \to \mathbb{R}^{3\times 3}$, with

$$J_{B_i}(\eta_{B_i}) = \begin{bmatrix} 1 & 0 & \sin(\theta_{B_i}) \\ 0 & \cos(\phi_{B_i}) & -\cos(\theta_{B_i})\sin(\phi_{B_i}) \\ 0 & \sin(\phi_{B_i}) & \cos(\theta_{B_i})\cos(\phi_{B_i}) \end{bmatrix}.$$

The pose of the $i$th end-effector can be computed via

$$\begin{aligned} p_{E_i} &= p_{B_i} + R_{B_i}(\eta_{B_i})k_{p_i}(\alpha_i) \\ \eta_{E_i} &= k_{\eta_i}(\eta_{B_i}, \alpha_i), \end{aligned}$$

where $k_{p_i} : \mathbb{R}^{n\alpha_i} \to \mathbb{R}^3, k_{\eta_i} : \mathbb{T}^3 \times \mathbb{R}^{n\alpha_i} \to \mathbb{T}^3$ are smooth functions representing the forward kinematics of the robotic arm (Siciliano and Khatib, 2008). Then, $v_i$ can be computed as

$$\begin{aligned} v_i &= \begin{bmatrix} \dot{p}_{E_i} \\ \omega_{E_i} \end{bmatrix} \\ &= \begin{bmatrix} \dot{p}_{B_i} - S\Big(R_{B_i}(\eta_{B_i})k_{p_i}(\alpha_i)\Big)\omega_{B_i} + R_{B_i}(\eta_{B_i})\frac{\partial k_{p_i}(\alpha_i)}{\partial \alpha_i}\dot{\alpha}_i \\ \omega_{B_i} + R_{B_i}(\eta_{B_i})J_{A_i}(\alpha_i)\dot{\alpha}_i \end{bmatrix} \end{aligned} \tag{5}$$

where $J_{A_i} : \mathbb{R}^{n\alpha_i} \to \mathbb{R}^{3\times n\alpha_i}$ is the angular Jacobian of the robotic arm with respect to the agent's base. The differential kinematics (5) can be written as

$$v_i = \begin{bmatrix} \dot{p}_{E_i} \\ \omega_{E_i} \end{bmatrix} = J_i(q_i)\dot{q}_i, \tag{6}$$

where $J_i : \mathbb{R}^{n_i} \to \mathbb{R}^{6\times n_i}$ is the agent Jacobian matrix, with

$$J_i(q_i) = \begin{bmatrix} I_3 & -S(R_{B_i}k_{p_i})J_{B_i} & R_{B_i}\frac{\partial k_{p_i}}{\partial \alpha_i} \\ 0_{3\times 3} & J_{B_i} & R_{B_i}J_{A_i} \end{bmatrix}, \tag{7}$$

where we have omitted the argument dependencies for brevity.

*Remark 1* Note that $J_{B_i}(\eta_{B_i})$ and $J_i(q_i)$ become singular when $\theta_{B_i} = \pm\frac{\pi}{2}$ and at kinematic singularities, respectively. Nevertheless, we assume that the agents will not operate close to a) kinematic singularities and b) configurations with $\theta_{B_i} = \pm\frac{\pi}{2}$ and therefore $J_{B_i}(\eta_{B_i})$ and $J_i(q_i)$ are always nonsingular. This assumption is valid in the case of mobile vehicles moving in the $x$-$y$ plane, where $\phi_{B_i} = \theta_{B_i} = 0$ in an appropriate reference frame. The same holds for aerial vehicles (e.g. quadrotors) with coupled kinematics, since $\phi_{B_i}, \theta_{B_i} \neq 0$ would result in motion in the $x$-$y$ directions. Avoidance of kinematic singularities is not taken into account in this work and is left for future considerations. It also holds that $J_i(q_i)$ is continuously differentiable away from kinematic singularities.

The joint-space dynamics for agent $i \in \mathcal{N}$ can be computed using the Lagrangian formulation as in (Lippiello and Ruggiero, 2012):

$$\begin{aligned} B_i(q_i)\ddot{q}_i + N_i(q_i,\dot{q}_i)\dot{q}_i + g_{q_i}(q_i) + f_{q_i}(q_i,\dot{q}_i) + w_{q_i}(t) = \\ \tau_i - J_i^T(q_i)\lambda_i, \end{aligned} \tag{8}$$

where $B_i : \mathbb{R}^{n_i} \to \mathbb{R}^{n_i\times n_i}$ is the joint-space positive definite inertia matrix, $N_i : \mathbb{R}^{n_i} \times \mathbb{R}^{n_i} \to \mathbb{R}^{n_i\times n_i}$ represents the joint-space Coriolis matrix, $g_{q_i} : \mathbb{R}^{n_i} \to \mathbb{R}^{n_i}$ is the joint-space gravity vector, $f_{q_i} : \mathbb{R}^{n_i} \times \mathbb{R}^{n_i} \to \mathbb{R}^{n_i}$ is a vector field representing model uncertainties and $w_{q_i} : \mathbb{R}_{\geq 0} \to \mathbb{R}^{n_i}$ is a bounded vector representing external disturbances. The aforementioned vector fields are smooth and unknown; $\lambda_i \in \mathbb{R}^6$ is the generalized force vector that agent $i$ exerts on the object and $\tau_i \in \mathbb{R}^{n_i}$ is the vector of generalized joint-space inputs, with $\tau_i = [\lambda_{B_i}^T, \tau_{\alpha_i}^T]^T$, where $\lambda_{B_i} = [f_{B_i}^T, \mu_{B_i}^T]^T \in \mathbb{R}^6$ is the generalized force vector on the center of mass of the agent's base and $\tau_{\alpha_i} \in \mathbb{R}^{n\alpha_i}$ are the torque inputs of the robotic arms' joints. By inverting (8) and using (6) and its derivative, we can obtain the task-space agent dynamics (Siciliano and Khatib, 2008):

$$\begin{aligned} M_i(q_i)\dot{v}_i + C_i(q_i,\dot{q}_i)v_i + g_i(q_i) + f_i(q_i,\dot{q}_i) + w_i(q_i,t) = \\ u_i - \lambda_i, \end{aligned} \tag{9}$$

with the corresponding task-space terms (Siciliano and Khatib, 2008), which are continuously differentiable, in view of the continuous differentiability of $J_i(q_i)$ and the smoothness of the joint-spae terms. The task-space input wrench $u_i$ can be translated to the joint space inputs $\tau_i \in \mathbb{R}^{n_i}$ via $\tau_i = J_i^T(q_i)u_i + (I_{n_i} - J_i^T(q_i)\bar{J}_i^T(q_i))\tau_{i_0}$, where $\bar{J}_i$ is a generalized inverse of $J_i$ (Siciliano and Khatib, 2008). The term $\tau_{i_0}$ concerns over-actuated agents and does not contribute to end-effector forces.

### 3.1.2 *Object Dynamics*

Regarding the object, we denote as $x_O \in \mathbb{M}$, $v_O \in \mathbb{R}^6$ the pose and velocity of the object's center of mass, with $x_O = [p_O^T, \eta_O^T]^T$, $\eta_O = [\phi_O, \theta_O, \psi_O]^T$ and $v_O = [\dot{p}_O^T, \omega_O^T]^T$. The second order dynamics of the object are given by:

$$\dot{x}_O = J_{O_r}^{-1}(x_O)v_O \tag{10a}$$

$$M_O(x_O)\dot{v}_O + C_O(x_O,v_O)v_O + g_O(x_O) + w_O(t) = \lambda_O, \tag{10b}$$

where $M_O : \mathbb{M} \to \mathbb{R}^{6\times 6}$ is the positive definite inertia matrix, $C_O : \mathbb{M} \times \mathbb{R}^6 \to \mathbb{R}^{6\times 6}$ is the Coriolis matrix, $g_O : \mathbb{M} \to \mathbb{R}^6$ is the gravity vector and $w_O : \mathbb{R}_{\geq 0} \to \mathbb{R}^6$ is a bounded vector representing external disturbances. Similarly to (9), all aforementioned vector fields are smooth and unknown. In addition, $J_{O_r} : \mathbb{M} \to \mathbb{R}^{6\times 6}$ is the object representation Jacobian $J_{O_r}(x_O) = \mathrm{diag}\{I_3, J_{O_{r,\theta}}(x_O)\}$, with

$$J_{O_{r,\theta}}(x_O) = \begin{bmatrix} 1 & 0 & \sin(\theta_O) \\ 0 & \cos(\phi_O) & -\cos(\theta_O)\sin(\phi_O) \\ 0 & \sin(\phi_O) & \cos(\theta_O)\cos(\phi_O) \end{bmatrix},$$

which is singular when $\theta_O = \pm\frac{\pi}{2}$. In the sequel, however, we will guarantee that the object avoids such configurations. Finally, $\lambda_O \in \mathbb{R}^6$ is the force vector acting on the object's center of mass.

### 3.1.3 *Coupled Dynamics*

In view of Fig. 2, we have that

$$p_{E_i} = p_O + p_{E_i/O} = p_O + R_{E_i}(q_i)p^{E_i}_{E_i/O} = p_O + R_O(\eta_O)p^{O}_{E_i/O}, \tag{11a}$$

$$\eta_{E_i} = \eta_O + \eta_{E_i/O}, \tag{11b}$$

$\forall i \in \mathcal{N}$, where $p^{E_i}_{E_i/O}$ represents the constant distance and $\eta_{E_i/O}$ the relative orientation offset between the $i$th agent's end-effector and the object's center of mass, which are considered known, as dictated above. Moreover, $R_{E_i} : \mathbb{R}^{n_i} \to SO(3)$ and $R_O : \mathbb{T}^3 \to SO(3)$ are the rotation matrices associated with the orientation of the $i$th end-effector and the object's center of mass, respectively. The grasp rigidity implies that $\omega_{E_i} = \omega_O$, $\forall i \in \mathcal{N}$. Therefore, by differentiating (11a), we obtain

$$v_i = J_{O_i}(q_i)v_O, \tag{12}$$

which yields

$$\dot{v}_i = J_{O_i}(q_i)\dot{v}_O + \dot{J}_{O_i}(q_i)v_O, \tag{13}$$

where $J_{O_i} : \mathbb{R}^{n_i} \to \mathbb{R}^{6\times 6}$ is a smooth mapping representing the Jacobian from the object to the $i$-th agent:

$$J_{O_i}(q_i) = \begin{bmatrix} I_3 & S(p_{O/E_i}(q_i)) \\ 0_{3\times 3} & I_3 \end{bmatrix}, \tag{14}$$

and is always full rank.

*Remark 2* Since the geometric object parameters $p^{E_i}_{E_i/O}$ and $\eta_{E_i/O}$ are known, each agent can compute $p_O, \eta_O$ and $v_O$ simply by inverting (11) and (12), respectively, without employing any sensory data.

The kineto-statics duality (Siciliano and Khatib, 2008) along with the grasp rigidity suggest that the force $\lambda_O$ acting on the object center of mass and the generalized forces $\lambda_i, i \in \mathcal{N}$, exerted by the agents at the contact points are related through

$$\lambda_O = G^T(q)\bar{\lambda}, \tag{15}$$

where $\bar{\lambda} = [\lambda_1^T, \cdots, \lambda_N^T]^T \in \mathbb{R}^{6N}$ and $G : \mathbb{R}^n \to \mathbb{R}^{6N\times 6}$ is the grasp matrix, with $G(q) = [J^T_{O_1}(q_1), \cdots, J^T_{O_N}(q_N)]^T$.

Next, we substitute (12) and (13) in (9) and we obtain in vector form after rearranging terms:

$$\bar{\lambda} = \bar{u} - \bar{M}(q)G(q)\dot{v}_O - (\bar{M}(q)\dot{G}(q) + \bar{C}(q,\dot{q})G(q))v_O - \bar{g}(q) - \bar{f}(q,\dot{q}) - \bar{w}(q,t) \tag{16}$$

where we have used the stack forms $\bar{M} = \text{diag}\{[M_i]_{i\in\mathcal{N}}\}$, $\bar{C} = \text{diag}\{[C_i]_{i\in\mathcal{N}}\}$, $\bar{g} = [g_1^T, \ldots, g_N^T]^T$, $\bar{f} = [f_1^T, \ldots, f_N^T]^T$, $\bar{u} = [u_1^T, \ldots, u_N^T]^T$ and $\bar{w} = [w_1^T, \ldots, w_N^T]^T$. By substituting (16) and (10) in (15) and by exploiting the dependence of $x_O$ on $q$ from (11), we obtain the coupled dynamics:

$$\widetilde{M}(q)\dot{v}_O + \widetilde{C}(q,\dot{q})v_O + \widetilde{h}(q,\dot{q}) + \widetilde{w}(q,t) = G^T(q)\bar{u}, \tag{17}$$

where

$$\widetilde{M}(q) = M_O(q) + G^T(q)\bar{M}(q)G(q) \tag{18a}$$

$$\widetilde{C}(q,\dot{q}) = C_O(q,\dot{q}) + G^T(q)\bar{M}(q)\dot{G}(q) + G^T(q)\bar{C}(q,\dot{q})G(q) \tag{18b}$$

$$\widetilde{h}(q,\dot{q}) = g_O(q) + G^T(q)\bar{g}(q) + G^T(q)\bar{f}(q,\dot{q}) \tag{18c}$$

$$\widetilde{w}(q,t) = w_O(t) + G^T(q)\bar{w}(q,t) \tag{18d}$$

Notice from (18a) that $\widetilde{M}$ is a positive definite matrix, owing to the positive definiteness of $M_O$ and $M_i, \forall i \in \mathcal{N}$, and the full column rank of $G$. Moreover, $\widetilde{M}(q), \widetilde{C}(q,\dot{q}), \widetilde{h}(q,\dot{q})$ are continuously differentiable in their arguments in singularity-free regions, and $\widetilde{w}(q,t)$ is continuously differentiable in $q$ and bounded in $t$ due to the continuous differentiability of $J_i(q_i)$ and the boundedness of $w_O(t)$ and $w_{q_i}(t), \forall i \in \mathcal{N}$.

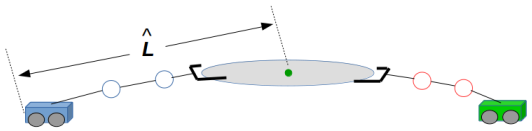


**Fig. 3** An example of the system shown in Fig. 2 in the configuration that produces $\hat{L}$.

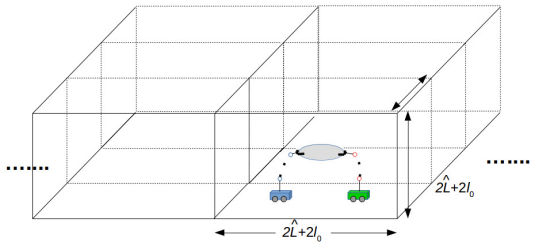


**Fig. 4** The workspace partition according to the bounding box of the coupled system.

## 3.2 Workspace Partition

As mentioned in Section 1, we are interested in designing a well-defined abstraction of the coupled object-agents system, so that we can define MITL formulas over certain properties in a discrete set of regions of the workspace. Therefore, we provide now a partition of $\mathcal{W}$ into cell regions. We denote as $\mathcal{S}_q$ the set that consists of all points $p_s \in \mathcal{W}$ that physically belong to the coupled system, i.e., they consist part of either the volume of the agents or the volume of the object. Note that these points depend on the actual value of $q$. We further define the constant $\hat{L} \geq \sup_{q\in\mathbb{R}^n,\, p_s\in\mathcal{S}_q} d(p_s, p_O(q))$, where, with a slight abuse of notation and in view of (11) and the forward kinematics of the agents, we express $p_O$ as

a function of $q$. Note that, although the explicit computation of $\mathcal{S}_q$ may not be possible, $\hat{L}$ is an upper bound of the maximum distance between the object center of mass and a point in the coupled system's volume over all possible configurations $q$, and thus, it can be measured. For instance, Fig. 3 shows $\hat{L}$ for the system of Fig. 2. It is straightforward to conclude that

$$p_s \in \mathcal{B}(p_o(q),\hat{L}), \forall p_s \in \mathcal{S}_q, q \in \mathbb{R}^n. \tag{19}$$

Next, we partition the workspace $\mathcal{W}$ into $R$ equally sized rectangular regions $\Pi = \{\pi_1,\ldots,\pi_R\}$, whose geometric centers are denoted as $p^c_{\pi_j} \in \mathcal{W}, j \in \{1,\ldots,R\}$. The length of the region sides is set to $D = 2\hat{L}+2l_0$, where $l_0$ is an arbitrary positive constant. Hence, each region $\pi_j$ can be formally defined as follows:

$$\pi_j = \{p \in \mathcal{W} \text{ s.t. } (p)_k \in [(p^c_{\pi_j})_k - \hat{L} - l_0, (p^c_{\pi_j})_k + \hat{L} + l_0), \\ \forall k \in \{x,y,z\}\},$$

with $d(p^c_{\pi_{j+1}}, p^c_{\pi_j}) = (2\hat{L}+2l_0), \forall j \in \{1,\ldots,R-1\}$, and $(p^c_{\pi_j})_z = \hat{L}+l_0, \forall j \in \{1,\ldots,R\}$; $(a)_k, k \in \{x,y,z\}$, denotes the $k$-th coordinate of $a = [(a)_x,(a)_y,(a)_z]^T \in \mathbb{R}^3$. An illustration of the aforementioned partition is depicted in Fig. 4.

Note that each $\pi_j$ is a uniformly bounded and convex set and also $\pi_j \cap \pi_{j'} = \emptyset, \forall j,j' \in \{1,\ldots,R\}$ with $j \neq j'$. We also define the neighborhood $\mathcal{D}$ of region $\pi_j$ as the set of its adjacent regions, i.e., $\mathcal{D}(\pi_j) = \{\pi_{j'} \in \Pi \text{ s.t. } d(p^c_{\pi_j}, p^c_{\pi_{j'}}) = (2\hat{L}+2l_0)\}$, which is symmetric, i.e., $\pi_{j'} \in \mathcal{D}(\pi_j) \Leftrightarrow \pi_j \in \mathcal{D}(\pi_{j'})$.

To proceed we need the following definitions regarding the timed transition of the coupled system between two regions $\pi_j, \pi_{j'}$:

**Definition 7** The coupled object-agents system is in region $\pi_j$ at a configuration $q$, denoted as $\mathcal{A}(q) \in \pi_j$, if and only if the following hold:

1. $p_s \in \pi_j, \forall p_s \in \mathcal{S}_q$
2. $d(p_o(q), p^c_{\pi_j}) < l_0$.

**Definition 8** Assume that $\mathcal{A}(q(t_0)) \in \pi_j, j \in \{1,\ldots,R\}$, for some $t_0 \in \mathbb{R}_{\geq 0}$. Then, there exists a transition for the coupled object-agents system from $\pi_j$ to $\pi_{j'}, j' \in \{1,\ldots,R\}$ with time duration $\delta t_{j,j'} \in \mathbb{R}_{\geq 0}$, denoted as $\pi_j \xrightarrow{\mathcal{T}} \pi_{j'}$, if and only if there exists a bounded control trajectory $\bar{u}$ in (17), such that the following hold:

1. $\mathcal{A}(q(t_0+\delta t_{j,j'})) \in \pi_{j'}$,
2. $p_s \in \pi_j \cup \pi_{j'}, \forall p_s \in \mathcal{S}_q, t \in [t_0, t_0+\delta t_{j,j'}]$.

Note that the entire system object-agents must remain in $\pi_j, \pi_{j'}$ during the transition and therefore the requirement $\pi_{j'} \in \mathcal{D}(\pi_j)$ is implicit in Definition 8.

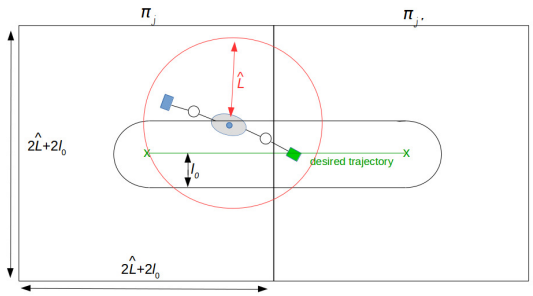


**Fig. 5** Top view of a transition between two adjacent regions $\pi_j$ and $\pi_{j'}$. Since $p_o \in \mathcal{B}(p_{j,j'}(t), l_0)$, we conclude that $p_s \in \mathcal{B}(p_o,\hat{L}) \subset \mathcal{B}(p_{j,j'}(t), l_0+\hat{L}) \subset \pi_j \cup \pi_{j'}$.

### 3.3 Specification

Given the workspace partition, we can introduce a set of atomic propositions $\mathcal{AP}$ for the object, which are expressed as Boolean variables that correspond to properties of interest in the regions of the workspace (e.g., "Obstacle region", "Goal region"). Formally, the labeling function $\mathcal{L}: \Pi \to 2^{\mathcal{AP}}$ assigns to each region $\pi_j$ the subset of the atomic propositions $\mathcal{AP}$ that are true in $\pi_j$.

**Definition 9** Given a time trajectory $q(t), t \geq 0$, a *timed sequence* of $q$ is the infinite sequence $\beta = (q(t_1),t_1)(q(t_2),t_2)\ldots$, with $t_m \in \mathbb{R}_{\geq 0}, t_{m+1} > t_m$ and $\mathcal{A}(q(t_m)) \in \pi_{j_m}, j_m \in \{1,\ldots,R\}, \forall m \in \mathbb{N}$. The *timed behavior* of $\beta$ is the infinite sequence $\sigma_\beta = (\sigma_1,t_1)(\sigma_2,t_2)\ldots$, with $\sigma_m \in 2^{\mathcal{AP}}, \sigma_m \in \mathcal{L}(\pi_{j_m})$ for $\mathcal{A}(q(t_m)) \in \pi_{j_m}, j_m \in \{1,\ldots,R\}, \forall m \in \mathbb{N}$, i.e., the set of atomic propositions that are true when $\mathcal{A}(q(t_m)) \in \pi_{j_m}$.

**Definition 10** The timed run $\beta$ satisfies an MITL formula $\phi$ if and only if $\sigma_\beta \models \phi$.

We are now ready to state the problem treated in this paper.

**Problem 1** Given $N$ agents rigidly grasping an object in $\mathcal{W}$ subject to the coupled dynamics (17), the workspace partition $\Pi$ such that $\mathcal{A}(q(0)) \in \pi_{j_0}, j_0 \in \{1,\ldots,R\}$, a MITL formula $\phi$ over $AP$ and the labeling function $\mathcal{L}$, derive a control strategy that achieves a timed sequence $\beta$ which yields the satisfaction of $\phi$.

## 4 Main Results

### 4.1 Control Design

The first ingredient of the proposed solution is the design of a decentralized control protocol $\bar{u}$ such that a transition relation between two adjacent regions according to Definition 8 is established. Assume, therefore, that $\mathcal{A}(q(t_0)) \in \pi_j, j \in \{1,\ldots,R\}$ for some $t_0 \in \mathbb{R}_{\geq 0}$. We aim to find a bounded $\bar{u}$, such that $\mathcal{A}(q(t_0+\delta t_{j,j'})) \in \pi_{j'}$, with $\pi_{j'} \in \mathcal{D}(\pi_j)$, and

$p_s \in \pi_j \cup \pi_{j'}, \forall p_s \in \mathcal{S}_q, t \in [t_0, t_0 + \delta t_{j,j'}]$, for a predefined arbitrary constant $\delta t_{j,j'} \in \mathbb{R}_{\geq 0}$ corresponding to the transition $\pi_j \xrightarrow{\mathcal{T}} \pi_{j'}$.

The first step is to associate to the transition a smooth and bounded trajectory with bounded time derivative, defined by the line segment that connects $p^c_{\pi_j}$ and $p^c_{\pi_{j'}}$, i.e. define $p_{j,j'} : [t_0, \infty) \to \mathbb{R}^3$, such that $p_{j,j'}(t_0) = p^c_{\pi_j}, p_{j,j'}(t) = p^c_{\pi_{j'}}, \forall t \geq t_0 + \delta t_{j,j'}$ and

$$\mathcal{B}(p_{j,j'}(t), \hat{L} + l_0) \subset \pi_j \cup \pi_{j'}, \ \ \forall t \geq t_0. \tag{20}$$

An example of $p_{j,j'}$ is

$$p_{j,j'}(t) = \begin{cases} \dfrac{p^c_{\pi_{j'}} - p^c_{\pi_j}}{\delta t_{j,j'}} t + \dfrac{p^c_{\pi_j}(\delta t_{j,j'} - 1) - p^c_{\pi_{j'}}}{\delta t_{j,j'}} t_0, & t \in T_1 \\ p^c_{\pi_{j'}}, & t \in T_2 \end{cases}, \tag{21}$$

where $T_1 = [t_0, t_0 + \delta t_{j,j'}), T_2 = [t_0 + \delta t_{j,j'}, \infty)$. The intuition behind the solution of Problem 1 via the definition of $p_{j,j'}$ is the following: if we guarantee that the object's center of mass stays $l_0$-close to $p_{j,j'}$, i.e., $d(p_O(t), p_{j,j'}(t)) < l_0, \forall t \geq t_0$, then $d(p_O(t_0 + \delta t_{j,j'}), p^c_{\pi_{j'}}) < l_0$ and, by invoking (19) and (20), we obtain $p_s \in \mathcal{B}(p_O(t), \hat{L}) \subset \mathcal{B}(p_{j,j'}(t), \hat{L} + l_0) \subset \pi_j \cup \pi_{j'}, \forall p_s \in \mathcal{S}_q, t \geq t_0$ (and therefore $t \in [t_0, t_0 + \delta t_{j,j'}]$), and thus the requirements of Definition 8 for the transition relation are met. Fig. 5 illustrates the aforementioned reasoning.

Along with $p_{j,j'}$, we consider that the object has to comply with certain specifications associated with its orientation. Therefore, we also define a smooth and bounded orientation trajectory $\eta_{j,j'} = [\phi_{j,j'}, \theta_{j,j'}, \psi_{j,j'}]^T : [t_0, \infty) \to \mathbb{T}^3$ with bounded time derivative, that has to be tracked by the object's center of mass. We choose $\theta_{j,j'}(t) \in [-\theta^*, \theta^*] \subset (-\frac{\pi}{2}, \frac{\pi}{2}), \forall t \in \mathbb{R}_{\geq 0}$, with $\theta^* \in (0, \frac{\pi}{2})$, so as to ensure the singularity avoidance of $J_{o_r}(x_O)$. We form, therefore, the desired pose trajectory $x_{j,j'} : [t_0, \infty) \to \mathbb{M}$, with $x_{j,j'}(t) = [p^T_{j,j'}(t), \eta^T_{j,j'}(t)]^T$. In case of multiple consecutive transitions $\ldots \pi_h \xrightarrow{\mathcal{T}} \pi_j \xrightarrow{\mathcal{T}} \pi_{j'} \xrightarrow{\mathcal{T}} \pi_{h'} \ldots$ over the intervals $\ldots, \delta t_{h,j}, \delta t_{j,j'}, \delta t_{j',h'}, \ldots$, the desired orientation trajectories $\ldots, \eta_{h,j}(t), \eta_{j,j'}(t), \eta_{j',h'}(t), \ldots$ must be continuous at the transition points, i.e., $\eta_{h,j}(t_0) = \eta_{j,j'}(t_0)$ and $\eta_{j,j'}(t_0 + \delta t_{j,j'}) = \eta_{j',h'}(t_0 + \delta t_{j,j'})$.

Therefore, Problem 1 is equivalent to a problem of trajectory tracking within certain bounds. Finally, we make the following assumption:

**Assumption 1** *The configuration of the object at $t = t_0$ does not result in a singular $J_{o_r}(x_O(t_0))$, i.e., $\theta_O(t_0) \in (-\frac{\pi}{2}, \frac{\pi}{2})$ and $\theta_{j,j'}(t)$ is chosen such that*

$$-\tfrac{\pi}{2} + \theta^* < \theta_O(t_0) - \theta_{j,j'}(t_0) < \tfrac{\pi}{2} - \theta^*.$$

We can now define the associated position and orientation errors $e_p = [e_{p_1}, e_{p_2}, e_{p_3}] \in \mathbb{R}^3, e_\eta = [e_{\eta_\phi}, e_{\eta_\theta}, e_{\eta_\psi}] \in \mathbb{T}^3$ as follows:

$$e_p = p_O - p_{j,j'}(t), \tag{22a}$$
$$e_\eta = \eta_O - \eta_{j,j'}(t), \tag{22b}$$

$\forall t \in [t_0, \infty)$.

A suitable methodology for the control design in hand is that of prescribed performance control, which is adapted in this work in order to achieve predefined transient and steady state response bounds for the pose errors. Following Section 2.3, prescribed performance characterizes the behavior where the aforementioned errors evolve strictly within a predefined region that is bounded by absolutely decaying functions of time, called performance functions. The mathematical expressions of prescribed performance are given by the inequalities:

$$-\rho_{p_k}(t) < e_{p_k}(t) < \rho_{p_k}(t), \ \ \forall k \in \{1,2,3\}, \tag{23a}$$
$$-\rho_{\eta_\ell}(t) < e_{\eta_\ell}(t) < \rho_{\eta_\ell}(t), \ \ \forall \ell \in \{\phi, \eta, \psi\}, \tag{23b}$$

$\forall t \in [t_0, \infty)$, where $\rho_{p_k}, \rho_{\eta_l} : [t_0, \infty) \to \mathbb{R}_{>0}$ with

$$\rho_{p_k}(t) = (\rho^0_{p_k} - \rho^\infty_{p_k}) e^{-l_{p_k}(t - t_0)} + \rho^\infty_{p_k}, \ \ \forall k \in \{1,2,3\}, \tag{24a}$$
$$\rho_{\eta_\ell}(t) = (\rho^0_{\eta_\ell} - \rho^\infty_{\eta_\ell}) e^{-l_{\eta_\ell}(t - t_0)} + \rho^\infty_{\eta_\ell}, \ \ \forall \ell \in \{\phi, \theta, \psi\}, \tag{24b}$$

are designer-specified, smooth, bounded and decreasing positive functions of time with $l_{p_k}, l_{\eta_\ell}, \rho^\infty_{p_k}, \rho^\infty_{\eta_\ell}, k \in \{1,2,3\}, \ell \in \{\phi, \theta, \psi\}$ positive parameters incorporating the desired transient and steady state performance respectively, as described in Section 2.3.

Next, we propose a state feedback control protocol that does not incorporate any information on the agents' or the object's dynamics or the external disturbances and guarantees (23) for all $t \in [t_0, \infty)$ and hence $[t_0, t_0 + \delta t_{j,j'}]$, which, by appropriately selecting $\rho_{p_k}(t), \rho_{\eta_\ell}(t), k \in \{1,2,3\}, \ell \in \{\phi, \theta, \psi\}$ and given that $\mathcal{A}(q(t_0)) \in \pi_j$, guarantees a representation singularity-free (i.e., $\theta_O(t) \neq \frac{\pi}{2}, t \in [t_0, \infty)$) transition $\pi_j \xrightarrow{\mathcal{T}} \pi_{j'}$ with time duration of $\delta t_{j,j'}$, as will be clarified in the sequel.

Define first the stack pose error $e_s :\in \mathbb{M}$:

$$e_s = \begin{bmatrix} e_{s_1} \\ e_{s_2} \\ e_{s_3} \\ e_{s_4} \\ e_{s_5} \\ e_{s_6} \end{bmatrix} = \begin{bmatrix} e_{p_1} \\ e_{p_2} \\ e_{p_3} \\ e_{\eta_\phi} \\ e_{\eta_\theta} \\ e_{\eta_\psi} \end{bmatrix} = x_O - x_{j,j'}(t), \tag{25}$$

$\forall t \in [t_0, \infty)$, and perform the following steps:

**Step I-a**. Select the corresponding functions $\rho_{p_k}, \rho_{\eta_\ell}$ as in (24) with

(i) $\rho^0_{p_k} = \rho_{p_k}(t_0) = l_0,\ \forall k \in \{1,2,3\},\ \rho^0_{\eta_\theta} = \rho_{\eta_\theta}(t_0) = \frac{\pi}{2} - \theta^*,\ \rho^0_{\eta_\ell} = \rho_{\eta_\ell}(t_0) > |e_{\eta_\ell}(t_0)|, \forall \ell \in \{\phi, \psi\}$,
(ii) $l_{p_k}, l_{\eta_\ell} \in \mathbb{R}_{>0}, \forall k \in \{1,2,3\}, \ell \in \{\phi, \theta, \psi\}$,
(iii) $\rho^\infty_{p_k} \in (0, \rho^0_{p_k}),\ \rho^\infty_{\eta_\ell} \in (0, \rho^0_{\eta_\ell}),\ \forall k \in \{1,2,3\},\ \ell \in \{\phi, \theta, \psi\}$.

**Step I-b**. Define the normalized errors $\xi_s \in \mathbb{R}^6$:

$$\xi_s = \begin{bmatrix} \xi_{s_1} \\ \vdots \\ \xi_{s_6} \end{bmatrix} = \rho_s^{-1}(t) e_s, \tag{26}$$

where $\rho_s(t) = \text{diag}\{\rho_{p_1}(t), \rho_{p_2}(t), \rho_{p_3}(t), \rho_{\eta_\phi}(t), \rho_{\eta_\theta}(t), \rho_{\eta_\psi}(t)\} \in \mathbb{R}^{6\times 6}$, and design the reference velocity vector $v_{O,\text{des}} : (-1,1)^6 \times [t_0, \infty) \to \mathbb{R}^6$, with:

$$v_{O,\text{des}}(\xi_s, t) = \begin{bmatrix} \dot{p}_{O,\text{des}}(\xi_s, t) \\ \omega_{O,\text{des}}(\xi_s, t) \end{bmatrix} = -g_s J_{O_r}(x_O) \rho_s^{-1}(t) r_s(\xi_s) \varepsilon_s(\xi_s)$$
$$= -g_s J_{O_r}(\rho_s(t)\xi_s + x_{j,j'}(t)) \rho_s^{-1}(t) r_s(\xi_s) \varepsilon_s(\xi_s), \tag{27}$$

where $g_s$ is a positive scalar tunable gain and the signals $\varepsilon_s : (-1,1)^6 \to \mathbb{R}^6, r_s : (-1,1)^6 \to \mathbb{R}^6$ are defined as:

$$\varepsilon_s(\xi_s) = \begin{bmatrix} \varepsilon_{s_1}(\xi_{s_1}) \\ \vdots \\ \varepsilon_{s_6}(\xi_{s_6}) \end{bmatrix} = \begin{bmatrix} \ln\left(\frac{1+\xi_{s_1}}{1-\xi_{s_1}}\right) \\ \vdots \\ \ln\left(\frac{1+\xi_{s_6}}{1-\xi_{s_6}}\right) \end{bmatrix}, \tag{28}$$

$$r_s(\xi_s) = \text{diag}\left\{ \left[ \frac{\partial \varepsilon_{s_m}(\xi_{s_m})}{\partial \xi_{s_m}} \right]_{m\in\{1,\ldots,6\}} \right\}$$
$$= \text{diag}\left\{ \left[ \frac{2}{(1-\xi^2_{s_m})} \right]_{m\in\{1,\ldots,6\}} \right\}. \tag{29}$$

**Step II-a**. Define the velocity error vector $e_v \in \mathbb{R}^6$ with

$$e_v = \begin{bmatrix} e_{v_1} \\ \vdots \\ e_{v_6} \end{bmatrix} = v_O - v_{O,\text{des}}(\xi_s, t), \tag{30}$$

and select the corresponding positive performance functions $\rho_{v_m} : [t_0, \infty) \to \mathbb{R}_{>0}$ with $\rho_{v_m}(t) = (\rho^0_{v_m} - \rho^\infty_{v_m}) e^{-l_{v_m}(t-t_0)} + \rho^\infty_{v_m}$, such that $\rho^0_{v_m} > |e_{v_m}(t_0)|, l_{v_m} > 0$ and $\rho^\infty_{v_m} \in (0, \rho^0_{v_m})$, $\forall m \in \{1, \ldots, 6\}$.

**Step II-b**. Define the normalized velocity errors $\xi_v \in \mathbb{R}^6$:

$$\xi_v = \begin{bmatrix} \xi_{v_1} \\ \vdots \\ \xi_{v_6} \end{bmatrix} = \rho_v^{-1}(t) e_v, \tag{31}$$

where $\rho_v(t) = \text{diag}\{[\rho_{v_m}(t)]_{m\in\{1,\ldots,6\}}\}$. Next, we use the inverse kinematics of the agents to express $q$ as a function of $x_{E_i}$, $q_i = \kappa_i(x_{E_i})$ , where $\kappa_i : \mathbb{M} \to \mathbb{R}^{n_i}$ is a mapping that is at least twice continuously differentiable away from kinematic singularities[1], $\forall i \in \mathcal{N}$ (Siciliano and Khatib, 2008). By using (11), the latter can be written as

$$q_i = \widetilde{\kappa}_i(x_O) = \kappa_i\left( \begin{bmatrix} p_O + R_O(\eta_O) p^O_{E_i/O} \\ \eta_O + \eta_{E_i/O} \end{bmatrix} \right).$$

Next, by employing (25), and (26), we can write $q_i = \hat{\kappa}_i(\xi_s, t)$ $= \widetilde{\kappa}_i(\rho_s(t)\xi_s + x_{j,j'}(t))$, which is bounded in $t$ due to the boundedness of $\rho_s(t)$ and $x_{j,j'}(t), \forall t \geq t_0$. Finally, we design the distributed control protocol for each agent $i \in \mathcal{N}$ as $u_i : (-1,1)^6 \times (-1,1)^6 \times [t_0, \infty) \to \mathbb{R}^6$:

$$u_i(\xi_s, \xi_v, t) = -c_i g_v \left( J^{-1}_{O_i}(q_i) \right)^T \rho_v^{-1}(t) r_v(\xi_v) \varepsilon_v(\xi_v),$$
$$= -c_i g_v \left( J^{-1}_{O_i}(\hat{\kappa}_i(\xi_s, t)) \right)^T \rho_v^{-1}(t) r_v(\xi_v) \varepsilon_v(\xi_v), \tag{32}$$

where $J_{O_i}$ as defined in (14), $g_v$ is a positive scalar tunable gain, and $c_i$ are predefined load sharing coefficients satisfying $\sum_{i\in\mathcal{N}} c_i = 1$ and $0 \leq c_i \leq 1, \forall i \in \mathcal{N}$. The signals $\varepsilon_v : (-1,1)^6 \to \mathbb{R}^6$ and $r_v : (-1,1)^6 \to \mathbb{R}^{6\times 6}$ are defined as:

$$\varepsilon_v(\xi_v) = \begin{bmatrix} \varepsilon_{v_1}(\xi_{v_1}) \\ \vdots \\ \varepsilon_{v_6}(\xi_{v_6}) \end{bmatrix} = \begin{bmatrix} \ln\left(\frac{1+\xi_{v_1}}{1-\xi_{v_1}}\right) \\ \vdots \\ \ln\left(\frac{1+\xi_{v_6}}{1-\xi_{v_6}}\right) \end{bmatrix}, \tag{33}$$

$$r_v(\xi_v) = \text{diag}\left\{ \left[ \frac{\partial \varepsilon_{v_m}(\xi_{v_m})}{\partial \xi_{v_m}} \right]_{m\in\{1,\ldots,6\}} \right\}$$
$$= \text{diag}\left\{ \left[ \frac{2}{(1-\xi^2_{v_m})} \right]_{m\in\{1,\ldots,6\}} \right\}. \tag{34}$$

The control law (32) can be written in vector form:

$$\bar{u}(\xi_s, \xi_v, t) = \begin{bmatrix} u_1(\xi_s, \xi_v, t) \\ \vdots \\ u_N(\xi_s, \xi_v, t) \end{bmatrix} = U_j^{j'}$$
$$= -C_g G^*(\hat{\kappa}(\xi_s, t)) \rho_v^{-1}(t) r_v(\xi_v) \varepsilon_v(\xi_v), \tag{35}$$

where $\hat{\kappa}(\xi_s, t) = [\hat{\kappa}_1^T(\xi_s, t), \ldots, \hat{\kappa}_N^T(\xi_s, t)]^T \in \mathbb{R}^{Nn_i}$, $G^*(q) = [J^{-1}_{O_1}(q_1), \ldots, J^{-1}_{O_N}(q_N)]^T \in \mathbb{R}^{6N\times 6}, C_g = g_v \text{diag}\{[c_i I_6]_{i\in\mathcal{N}}\} \in \mathbb{R}^{6N\times 6N}$, and the notation $U_j^{j'}$ stands for the transition from $\pi_j$ to $\pi_{j'}$.

The aforementioned control protocol for the transition $\pi_j \xrightarrow{\mathcal{T}} \pi_{j'}$ is summarized in Algorithm 1.

*Remark 3* Notice by (27) and (32) that the proposed control protocol is distributed in the sense that each agent needs feedback only from the state of the object's center of mass, which can be obtained by (11) and (12), as discussed in

[1] We focus on robotic structures where such a function exists, which constitute the majority of cases.

**Algorithm 1** Transition Algorithm

1: Compute trajectory $x_{j,j'}(t)$ associated to $\pi_j \xrightarrow{\mathcal{T}} \pi_{j'}$
2: Compute pose error $e_s = x_O - x_{j,j'}(t)$
3: Define pose performance functions $\rho_s(t)$
4: Define the pose normalized error $\xi_s = \rho_s^{-1}(t)e_s$
5: Define reference velocity $v_{O,\text{des}}(\xi_s,t)$
6: Compute velocity error $e_v = v_O - v_{O,\text{des}}(\xi_s,t)$
7: Define velocity performance functions $\rho_v(t)$
8: Define the velocity normalized error $\xi_v = \rho_v^{-1}(t)e_v$
9: Compute distributed control laws $u_i(\xi_s,\xi_v,t), i \in \mathcal{N}$

Section 3.1.3. The parameters needed for the computation of $\rho_{p_k}(t), \rho_{\eta_\ell}(t), \rho_{v_m}(t), \forall k \in \{1,2,3\}$, $\ell \in \{\phi,\theta,\psi\}$, $m \in \{1,\dots,6\}$ as well as $c_i, g_s, g_v$ and $\eta_{j,j'}(t), i \in \mathcal{N}$, can be transmitted off-line to the agents. Moreover, the proposed control law does not incorporate any prior knowledge of the model nonlinearities/disturbances or force/torque measurements at the contact points. Furthermore, the proposed methodology results in a low complexity design. Notice that no hard calculations (neither analytic nor numerical) are required to output the proposed control signal, thus making its distributed implementation straightforward.

*Remark 4* We can also guarantee internal force regulation by including in (35) a vector of desired internal forces $f_{\text{int,d}} \in \mathbb{R}^{6N}$ that belongs to the nullspace of $G^T$, i.e., $f_{\text{int,d}} = (I_{6N} - \frac{1}{N}G^*(q)G^T(q))\hat{f}_{\text{int,d}}$, where $\hat{f}_{\text{int,d}}$ is a constant vector that can be transmitted off-line to the agents. Note though, that the computation of $G^*(q)G^T(q)$ by each agent requires knowledge of all grasping points $p_{E_i}$. This reduces to knowledge of the constant offsets $p^O_{E_i/O}$. Then, each agent $j \in \mathcal{N}$ can compute $p_{E_i}$ via $p_{E_i} = p_O + R_O(\eta_O)p^O_{E_i/O}, \forall i \in \mathcal{N}\backslash\{j\}$ (since agent $j$ can compute $R_O(\eta_O)$ and $p_O$ by inverting (11) for $i = j$). The constant offsets $p^O_{E_i/O}$ can be transmitted off-line to the agents, without the need of inter-agent on-line communication. Note that the vectors $p_{E_i}$ can also be obtained on-line via appropriate sensors (e.g., mounted cameras that recognize potential markers on the other agents' end-effectors), since all agents have the same inertial frame of reference $\{I\}$.

The next theorem summarizes the results of this section.

**Theorem 2** *Consider N agents rigidly grasping an object with unknown coupled dynamics* (17) *and* $\mathcal{A}(q(t_0)) \in \pi_j, j \in \{1,\dots,R\}$. *Then, the distributed control protocol* (25)-(34) *guarantees that* $\pi_j \xrightarrow{\mathcal{T}} \pi_{j'}$ *with time duration* $\delta t_{j,j'}$ *and all closed loop signals being bounded, and thus establishes a transition relation between* $\pi_j$ *and* $\pi_{j'}$ *for the coupled object-agents system, according to Definition 8.*

*Proof* By differentiating (26) and (31) with respect to time, we obtain

$$\dot{\xi}_s = \rho_s^{-1}(t)(\dot{e}_s - \dot{\rho}_s(t)\xi_s)$$
$$\dot{\xi}_v = \rho_v^{-1}(t)(\dot{e}_v - \dot{\rho}_v(t)\xi_v),$$

which, after substituting (17), (25), (30), and employing $q = \hat{\kappa}(\xi_s,t)$, becomes

$$\dot{\xi}_s = \rho_s^{-1}(t)\left(J_{O_r}^{-1}(\rho_s(t)\xi_s + x_{j,j'}(t))v_O - \dot{x}_{j,j'}(t) - \dot{\rho}_s(t)\xi_s\right) \tag{36a}$$

$$\dot{\xi}_v = \rho_v^{-1}(t)\Big\{\widetilde{M}^{-1}(\hat{\kappa}(\xi_s,t))\left[G^T(\hat{\kappa}(\xi_s,t))\bar{u} - \widetilde{w}(\hat{\kappa}(\xi_s,t),t)\right.$$
$$\left.-\widetilde{C}(\hat{\kappa}(\xi_s,t),\dot{\hat{\kappa}}(\xi_s,t))v_O - \widetilde{h}(\hat{\kappa}(\xi_s,t),\dot{\hat{\kappa}}(\xi_s,t))\right] - \dot{v}_{O,\text{des}}(\xi_s,t)$$
$$-\dot{\rho}_v(t)\xi_v\Big\}. \tag{36b}$$

By employing (27), (35) as well as the fact that $v_O = \rho_v(t)\xi_v + v_{O,\text{des}}(\xi_s,t)$ and $\sum_{i\in\mathcal{N}} c_i = 1$, we obtain from (36):

$$\dot{\xi}_s = h_s(\xi_s,t)$$
$$= -g_s\rho_s^{-1}(t)r_s(\xi_s)\varepsilon_s(\xi_s) + \rho_s^{-1}(t)\left[J_{O_r}^{-1}(\rho_s(t)\xi_s\right.$$
$$\left.+x_{j,j'}(t))\rho_v(t)\xi_v - \dot{x}_{j,j'}(t) - \dot{\rho}_s(t)\xi_s\right], \tag{37a}$$

$$\dot{\xi}_v = h_v(\xi_s,\xi_v,t)$$
$$= -g_v\rho_v^{-1}(t)\widetilde{M}^{-1}(\hat{\kappa}(\xi_s,t))\rho_v^{-1}(t)r_v(\xi_v)\varepsilon_v(\xi_v) -$$
$$\rho_v^{-1}(t)\Big\{\widetilde{M}^{-1}(\hat{\kappa}(\xi_s,t))\left[\widetilde{h}(\hat{\kappa}(\xi_s,t),\dot{\hat{\kappa}}(\xi_s,t)) + \widetilde{w}(\hat{\kappa}(\xi_s,t),t)\right.$$
$$\left.+\widetilde{C}(\hat{\kappa}(\xi_s,t),\dot{\hat{\kappa}}(\xi_s,t))(\rho_v(t)\xi_v + v_{O,\text{des}}(\xi_s,t))\right] + \dot{v}_{O,\text{des}}(\xi_s,t)$$
$$+\dot{\rho}_v(t)\xi_v\Big\}, \tag{37b}$$

where we implicitly use $\dot{v}_{O,\text{des}}(\xi_s,t) = \frac{\partial v_{O,\text{des}}(\xi_s,t)}{\partial \xi_s}h_s(\xi_s,t) + \frac{\partial v_{O,\text{des}}(\xi_s,t)}{\partial t}$ and $\dot{\hat{\kappa}}(\xi_s,t) = \frac{\partial \hat{\kappa}(\xi_s,t)}{\partial \xi_s}h_s(\xi_s,t) + \frac{\partial \hat{\kappa}(\xi_s,t)}{\partial t}$.

By defining the open and nonempty set $\Omega_\xi = \Omega_{\xi_s} \times \Omega_{\xi_v} \subset \mathbb{R}^{12}$ with $\Omega_{\xi_s} = \Omega_{\xi_v} = (-1,1)^6$, as well as $h : \Omega_\xi \times [t_0,\infty) \to \mathbb{R}^{12}$, we can write (37) in compact form:

$$\dot{\xi} = h(\xi,t) = \begin{bmatrix} h_s(\xi,t) \\ h_v(\xi,t) \end{bmatrix} \tag{38}$$

where $\xi = [\xi_s^T, \xi_v^T] \in \mathbb{R}^{12}$.

The proof continues in two main parts. Firstly, we guarantee that a unique maximal solution $\xi : [t_0,\tau_{\max}) \to \Omega_\xi$ of (38) exists, where $\tau_{\max} > t_0$. Then, we prove that all closed loop signals are bounded and that $\xi(t) \in \Omega'_\xi \subset \Omega_\xi, \forall t \in [t_0,\tau_{\max})$, where $\Omega'_\xi$ is compact, which leads by contradiction to the conclusion that $\tau_{\max} = \infty$ and the completion of the proof.

Since $\mathcal{A}(q(t_0)) \in \pi_j, j \in \{1,\dots,R\}$, Definition 7 implies that $d(p_O(q(t_0)), p^c_{\pi_j}) < l_0$. Also, $p_{j,j'}(t_0) = p^c_{\pi_j}$. Therefore, by choosing $\rho^0_{p_k} = l_0, \forall k \in \{1,2,3\}$ as well as $\rho^0_{\eta_\theta} = \frac{\pi}{2} - \theta^*$, $\rho^0_{\eta_\ell} > |e_{\eta_\ell}(t_0)|, \forall \ell \in \{\phi,\psi\}$ and owing to Assumption 1, we guarantee that $\xi_{s_m}(t_0) \in (-1,1), \forall m \in \{1,\dots,6\}$ and therefore $\xi_s(t_0) \in \Omega_{\xi_s}$. Furthermore, by selecting $\rho^0_{v_m} > |e_{v_m}(t_0)|$, $\forall m \in \{1,\dots,6\}$, we guarantee that $\xi_v(t_0) \in \Omega_{\xi_v}$ as well. Thus, we conclude that $\xi(t_0) \in \Omega_\xi$. Additionally, $h$ is continuous in $t$ and locally Lipschitz in $\xi$ over $\Omega_\xi$. To see that, note first from (36a) that $h_s(\xi_s,t)$ is continuously differentiable in $\xi_s$ over $(-1,1)^6$, due to the continuously differentiable functions $r_s(\xi_s), \varepsilon(\xi_s)$ over $(-1,1)^6$, as defined in (28)

and (29), respectively, as well as the continuous differentiability of $J_{O_r}(x_O)$ and its inverse $\forall \xi_{s_5} \in (-1,1)$ (note that the constraint $\xi_{s_5} \in (-1,1)$ implies $|\theta_O| < \frac{\pi}{2}$ due to the choice of the errors (22) and the performance function $\rho_{\eta_\theta}(t)$). Hence, we conclude that $h_s(\xi_s,t)$ is continuously differentiable and thus locally Lipschitz in $\xi_s$ over $(-1,1)^6$. Furthermore, it is straightforward to verify the continuous differentiability of $\dot{v}_{O,\mathrm{des}}(\xi_s,t)$ in $\xi_s$ over $(-1,1)^6$. In addition, the functions $\hat{\kappa}(\xi_s,t), \dot{\hat{\kappa}}(\xi_s,t)$ are continuously differentiable in $\xi_s$ away from kinematic singularities (which, as stated previously, we don't take into account in this work). Thus, the cont. differentiability of $r_v(\xi_v)$, $\varepsilon_v(\xi_v)$, $v_{O,\mathrm{des}}(\xi_s,t)$ over $(-1,1)^6$ in $\xi_v$ and $\xi_s$, respectively, as well as the smoothness of $\widetilde{M}^{-1}, \widetilde{C}, \widetilde{h}, \widetilde{w}$ render the function $h_v(\xi_s,\xi_v,t)$ continuously differentiable and hence locally Lipschitz in $\xi$ over the set $\Omega_\xi$.

Therefore, according to Theorem 1, there exists a maximal solution $\xi(t)$ of (38) on a time interval $[t_0,\tau_{\max})$ such that $\xi(t) \in \Omega_\xi, \forall t \in [t_0,\tau_{\max})$. Thus:

$$\xi_{s_m}(t) = \frac{e_{s_m}(t)}{\rho_{s_m}(t)} \in (-1,1), \tag{39a}$$

$$\xi_{v_m}(t) = \frac{e_{v_m}(t)}{\rho_{v_m}(t)} \in (-1,1), \tag{39b}$$

$\forall m \in \{1,\ldots,6\}, t \in [t_0,\tau_{\max})$, from which we conclude that $e_{s_m}(t)$ and $e_{v_m}(t)$ are bounded by $\rho_{s_m}(t)$ and $\rho_{v_m}(t)$, respectively. Therefore, the error vectors $\varepsilon_s(\xi_s)$ and $\varepsilon_v(\xi_v)$, as defined in (28) and (33), respectively, are well defined for all $t \in [t_0,\tau_{\max})$. Hence, consider the positive definite and radially unbounded function $V_s : \mathbb{R}^6 \to \mathbb{R}_{\geq 0}$ with $V_s(\varepsilon_s) = \frac{1}{2}\varepsilon_s^T\varepsilon_s$. Differentiation of $V_s$ yields $\dot{V}_s = \varepsilon_s^T(\xi_s) r_s(\xi_s)\dot{\xi}_s$ which, by substituting (37a) and employing the fact that $r_s(\xi_s), \rho_s(t)$ are diagonal, becomes:

$$\begin{aligned}\dot{V}_s = &- g_s \|r_s(\xi_s)\rho_s^{-1}(t)\varepsilon_s(\xi_s)\|^2 - \varepsilon_s^T(\xi_s) r_s(\xi_s)\rho_s^{-1}(t)\left[\dot{x}_{j,j'}(t)\right.\\ &\left. + \dot{\rho}_s(t)\xi_s - J_{O_r}^{-1}(\rho_s(t)\xi_s + x_{j,j'}(t))\rho_v(t)\xi_v\right],\end{aligned}$$

Note that $\rho_v(t), \dot{\rho}_s(t)$ as well as $x_{j,j'}(t), \dot{x}_{j,j'}(t)$are bounded by construction, $\forall t \in [t_0,\infty)$. Also, owing to (39), it holds that $\|\xi_s(t)\| \leq \sqrt{6}$ and $\|\xi_v(t)\| \leq \sqrt{6}$, $\forall t \in [t_0,\tau_{\max})$. Hence, the continuity of $J_{O_r}^{-1}$ implies that $J_{O_r}^{-1}(\rho_s(t)\xi_s(t) + x_{j,j'}(t))$ is also bounded by a constant independent of $\tau_{\max}$, $\forall t \in [t_0,\tau_{\max})$. Hence, $\dot{V}_s$ becomes:

$$\dot{V}_s \leq -g_s\|r_s(\xi_s)\rho_s^{-1}(t)\varepsilon_s(\xi_s)\|^2 + \|r_s(\xi_s)\rho_s^{-1}(t)\varepsilon_s(\xi_s)\|\bar{B}_s,$$

$\forall t \in [t_0,\tau_{\max})$, where $\bar{B}_s$ is an unknown positive constant, independent of $\tau_{\max}$, satisfying

$$\begin{aligned}\bar{B}_s \geq \|\dot{x}_{j,j'}(t) + \dot{\rho}_s(t)\xi_s - J_{O_r}^{-1}(\rho_s(t)\xi_s + \\ x_{j,j'}(t))\rho_v(t)\xi_v\|,\end{aligned} \tag{40}$$

$\forall t \in [t_0,\tau_{\max})$. Therefore, $\dot{V}_s$ is written as:

$$\dot{V}_s \leq -\|r_s(\xi_s)\rho_s^{-1}(t)\varepsilon_s(\xi_s)\|\left(g_s\|r_s(\xi_s)\rho_s^{-1}(t)\varepsilon_s(\xi_s)\| - \bar{B}_s\right),$$

$\forall t \in [t_0,\tau_{\max})$, from which we conclude that

$$\dot{V}_s < 0 \Leftrightarrow \|r_s(\xi_s)\rho_s^{-1}(t)\varepsilon_s(\xi_s)\| > \frac{\bar{B}_s}{g_s}. \tag{41}$$

Note from (24), (29) and (39a) that $\rho_{s_m}(t) < \rho_{s_m}^0$ and $r_{s_m}(\xi_{s_m}) > 1, \forall t \in [0,\tau_{\max})$. Therefore, (41) is equivalent to

$$\dot{V}_s < 0 \Leftrightarrow \|\varepsilon_s(\xi_s)\| > \frac{\bar{B}_s \max_{m\in\{1,\ldots,6\}}\{\rho_{s_m}^0\}}{g_s}, \tag{42}$$

which implies that

$$\begin{aligned}&\|\varepsilon_s(\xi_s(t))\| \leq \bar{\varepsilon}_s\\ &= \max\left\{\|\varepsilon_s(\xi_s(t_0))\|, \frac{\bar{B}_s \max_{m\in\{1,\ldots,6\}}\{\rho_{s_m}^0\}}{g_s}\right\},\end{aligned} \tag{43}$$

$\forall t \in [t_0,\tau_{\max})$. Also, by using $|\varepsilon_{s_m}(\xi_s(t))| \leq \|\varepsilon_s(\xi_s(t))\|$, $\forall m \in \{1,\ldots,6\}$, and the inverse logarithm function, we obtain from (28):

$$-1 < \frac{e^{-\bar{\varepsilon}_s}-1}{e^{-\bar{\varepsilon}_s}+1} = \underline{\xi}_s \leq \xi_{s_m}(t) \leq \bar{\xi}_s = \frac{e^{\bar{\varepsilon}_s}-1}{e^{\bar{\varepsilon}_s}+1} < 1 \tag{44}$$

$\forall t \in [t_0,\tau_{\max}), m \in \{1,\ldots,6\}$. Note that $\bar{\varepsilon}_s$ and hence $\bar{\xi}_s$ and $\underline{\xi}_s$ do not depend on $\tau_{\max}$. Therefore, due to (43) and (44), the reference velocity vector $v_{O,\mathrm{des}}(\xi_s,t)$, as defined in (27), remains bounded for all $t \in [t_0,\tau_{\max})$ by a bound independent of $\tau_{\max}$. Moreover, invoking $v_O = \rho_v(t)\xi_v + v_{O,\mathrm{des}}(\xi_s,t)$ and (39), we also conclude the boundedness of $v_O$ for all $t \in [t_0,\tau_{\max})$, independently of $\tau_{\max}$. Finally, differentiating $v_{O,\mathrm{des}}$ with respect to time and employing (37a), (39) and (44), we also conclude the boundedness of $\dot{v}_{O,\mathrm{des}}(\xi_s,t), \forall t \in [t_0,\tau_{\max})$, independently of $\tau_{\max}$.

Applying the aforementioned line of proof, we consider the positive definite and radially unbounded function $V_v : \mathbb{R}^6 \to \mathbb{R}$ with $V_v(\varepsilon_v) = \frac{1}{2}\varepsilon_v^T\varepsilon_v$. Differentiation of $V_v$ yields $\dot{V}_v = \varepsilon_v^T(\xi_v) r_v(\xi_v)\dot{\xi}_v$ which, by substituting (37a), becomes:

$$\begin{aligned}&\dot{V}_v = -g_v\varepsilon_v^T(\xi_v) r_v(\xi_v)\rho_v^{-1}(t)\widetilde{M}^{-1}(\hat{\kappa}(\xi_s,t))\rho_v^{-1}(t) r_v(\xi_v)\varepsilon_v(\xi_v) -\\ &\varepsilon_v^T(\xi_v) r_v(\xi_v)\rho_v^{-1}(t)\left\{\dot{\rho}_v(t)\xi_v + \widetilde{M}^{-1}(\hat{\kappa}(\xi_s,t))\left[\widetilde{h}(\hat{\kappa}(\xi_s,t),\dot{\hat{\kappa}}(\xi_s,t))\right.\right.\\ &\left.\left. + \widetilde{w}(\hat{\kappa}(\xi_s,t),t) + \widetilde{C}(\hat{\kappa}(\xi_s,t),\dot{\hat{\kappa}}(\xi_s,t))(\rho_v(t)\xi_v + v_{O,\mathrm{des}}(\xi_s,t))\right] +\right.\\ &\left.\dot{v}_{O,\mathrm{des}}(\xi_s,t)\right\}.\end{aligned} \tag{45}$$

Proceeding in a similar manner as with $\dot{V}_s$, we note that $\dot{\rho}_v(t)$ and $\xi_v$ are bounded by construction and due to (39b), respectively, by bounds independent of $\tau_{\max}$. Moreover, the functions $\hat{\kappa}(\xi_s,t), \dot{\hat{\kappa}}(\xi_s,t)$ are continuous functions of their arguments and, in view of their definitions and (37a), they are bounded in $t$ for all $t \geq t_0$ due to the boundedness of $\rho_s(t), \rho_v(t), \dot{\rho}_s(t), x_{j,j'}(t)$ and $\dot{x}_{j,j'}(t)$, $\forall t \geq t_0$. Thus, they are also bounded by bounds independent of $\tau_{\max}$. Hence, the continuity of the terms $\widetilde{M}^{-1}, \widetilde{C}, \widetilde{h}, \widetilde{w}$ as well the boundedness of $\widetilde{w}$ in $t$ (by assumption) dictates their boundedness for all $t \in [t_0,\tau_{\max})$, by bounds independent of $\tau_{\max}$. Finally,

$\dot{v}_{O,\text{des}}(\xi_s,t)$ was proven bounded for all $t \in [t_0, \tau_{\max})$, independently of $\tau_{\max}$. Using the aforementioned reasoning as well as the positive definiteness of $\widetilde{M}$ and therefore of $\widetilde{M}^{-1}$, $\dot{V}_v$ becomes

$$\dot{V}_v \leq -\|\rho_v^{-1}(t) r_v \varepsilon_v(\xi_v)\| \left( g_v \lambda_{\min}(\widetilde{M}^{-1}) \|\rho_v^{-1}(t) r_v \varepsilon_v(\xi_v)\| - \bar{B}_v \right) \tag{46}$$

$\forall t \in [t_0, \tau_{\max})$, where $\bar{B}_v$ is a positive constant independent of $\tau_{\max}$, satisfying

$$\bar{B}_v \geq \Big\| \widetilde{M}^{-1}(\hat{\kappa}(\xi_s,t)) \Big[ \widetilde{h}(\hat{\kappa}(\xi_s,t), \dot{\hat{\kappa}}(\xi_s,t)) + \widetilde{w}(\hat{\kappa}(\xi_s,t),t) + \widetilde{C}(\hat{\kappa}(\xi_s,t), \dot{\hat{\kappa}}(\xi_s,t))(\rho_v(t)\xi_v + v_{O,\text{des}}(\xi_s,t)) \Big] - \dot{v}_{O,\text{des}}(\xi_s,t) - \dot{\rho}_v(t)\xi_v \Big\|, \tag{47}$$

$\forall t \in [t_0, \tau_{\max})$. Therefore, we conclude that

$$\dot{V}_v < 0 \Leftrightarrow \|\rho_v^{-1}(t) r_v(\xi_v) \varepsilon_v(\xi_v)\| > \frac{\bar{B}_v}{\lambda_{\min}(\widetilde{M}^{-1}) g_v},$$

which is equivalent to

$$\dot{V}_v < 0 \Leftrightarrow \|\varepsilon_v(\xi_v)\| > \frac{\bar{B}_v \max_{m\in\{1,\ldots,6\}}\{\rho_{v_m}^0\}}{\lambda_{\min}(\widetilde{M}^{-1}) g_v}.$$

Hence, we deduce that

$$\|\varepsilon_v(\xi_v(t))\| \leq \bar{\varepsilon}_v = \max\left\{ \|\varepsilon_v(\xi_v(t_0))\|, \frac{\bar{B}_v \max_{m\in\{1,\ldots,6\}}\{\rho_{v_m}^0\}}{\lambda_{\min}(\widetilde{M}^{-1}) g_v} \right\}, \tag{48}$$

$\forall t \in [t_0, \tau_{\max})$. Furthermore, we obtain from (28) by taking the inverse logarithm:

$$-1 < \frac{e^{-\bar{\varepsilon}_v} - 1}{e^{-\bar{\varepsilon}_v} + 1} = \underline{\xi}_v \leq \xi_{v_m}(t) \leq \bar{\xi}_v = \frac{e^{\bar{\varepsilon}_v} - 1}{e^{\bar{\varepsilon}_v} + 1} < 1 \tag{49}$$

$\forall t \in [t_0, \tau_{\max}), m \in \{1,\ldots,6\}$, which also leads to the boundedness of the distributed control protocol (35).

Up to this point, what remains to be shown is that $\tau_{\max}$ can be extended to infinity. In this direction, notice by (44) and (49) that $\xi(t) \in \Omega'_\xi = \Omega'_{\xi_s} \times \Omega'_{\xi_v}, \forall t \in [t_0, \tau_{\max})$, where:

$$\Omega'_{\xi_s} = [\underline{\xi}_s, \bar{\xi}_s]^6, \;\; \Omega'_{\xi_v} = [\underline{\xi}_v, \bar{\xi}_v]^6$$

are nonempty and compact subsets of $\Omega_{\xi_s}$ and $\Omega_{\xi_v}$, respectively. Hence, assuming that $\tau_{\max} < \infty$ and since $\Omega'_\xi \subset \Omega_\xi$, Proposition 1 dictates the existence of a time instant $t' \in [t_0, \tau_{\max})$ such that $\xi(t') \notin \Omega'_\xi$, which is a clear contradiction. Therefore, $\tau_{\max} = \infty$. Thus, all closed loop signals remain bounded and moreover $\xi(t) \in \Omega'_\xi, \forall t \geq t_0$.

By multiplying (44) with $\rho_{s_m}(t)$, we obtain $|e_{s_m}(t)| < \rho_{s_m}(t), \forall m \in \{1,\ldots,6\}$ and thus $|e_{p_k}(t)| < l_0, \forall p \in \{1,2,3\}$, $t \in [t_0, \infty)$, since $\rho_{p_k}^0 = l_0, \forall k \in \{1,2,3\}$. Therefore, $p_O(q(t)) \in \mathcal{B}(p_{j,j'}(t), l_0), \forall t \geq t_0$ and, consequently, $p_O(q(t_0 + \delta t_{j,j'})) \in \mathcal{B}(p^c_{\pi_{j'}}, l_0)$, since $p_{j,j'}(t_0 + \delta t_{j,j'}) = p^c_{\pi_{j'}}$. Moreover, since $p_O(q(t)) \in \mathcal{B}(p_{j,j'}(t), l_0)$, we deduce that $\mathcal{B}(p_O(q(t)), \hat{L}) \subset \mathcal{B}(p_{j,j'}(t), l_0 + \hat{L})$ and invoking (19) and (20), we conclude that $p_s \in \pi_j \cup \pi_{j'}, \forall t \in [t_0, t_0 + \delta t_{j,j'}] \subset [t_0, \infty)$, and therefore a transition relation with time duration $\delta t_{j,j'}$ is successfully established. Finally, since $\rho^0_{\eta_\theta} = \rho_{\eta_\theta}(t_0) = \frac{\pi}{2} - \theta^*$ and $|e_{\eta_\theta}(t)| < \rho_{\eta_\theta}(t) \leq \rho_{\eta_\theta}(t_0), |\theta_{j,j'}(t)| < \theta^*, \forall t \in [t_0, \infty)$, we conclude that $|\theta_O(t)| < \frac{\pi}{2}, \forall t \in [t_0, \infty)$, ensuring thus the representation singularity-free transition $\pi_j \xrightarrow{\mathcal{T}} \pi_{j'}$.

*Remark 5* Instead of employing the control protocol (35) over $[t_0, \infty)$, we can define it over a finite time interval as $\bar{u}(\xi_s, \xi_v, [t_0, t_0 + \delta t_{j,j'}))$. In that case, it follows by the continuity of $d, p_O, p_{j,j'}$ that $\lim_{t\to(t_0+\delta t_{j,j'})^-} d(p_O(t), p_{j,j'}(t)) = d(p_O(t_0 + \delta t_{j,j'}), p^c_{\pi_{j'}})$ and therefore, the transition $\pi_j \xrightarrow{\mathcal{T}} \pi_{j'}$ with time duration $\delta t_{j,j'}$ is still achieved. Moreover, the predefined selection of $\delta t_{j,j'}$ for each transition $\pi_j \xrightarrow{\mathcal{T}} \pi_{j'}$ is related to the control capabilities of the agents, since smaller $\delta t_{j,j'}$ will produce larger, but still bounded, $v_{O,\text{des}}$ and $\bar{u}$.

*Remark 6* We can deduce from the aforementioned analysis that (43) and (48) hold without the need of adjusting the control gains $g_s, g_v$ to render the bounds $\bar{\varepsilon}_s, \bar{\varepsilon}_v$ arbitrary small. The uncertainties in the nonlinear coupled model (17) affect only the size of $\bar{\varepsilon}_v$ through $\bar{B}_v$ (see (47)) and not the stability properties. Hence, the actual performance of the system is determined by the performance functions $\rho_{s_m}(t), \rho_{v_m}(t), m \in \{1,\ldots,6\}$ and is robust against model uncertainties and external disturbances.

*Remark 7* It should be noted that the selection of the control gains affects the behavior of the errors in the performance function envelope as well as the control input characteristics. To this end, fine tuning of the control gains might be needed in real-time scenarios, to retain the required control input signal within the feasible range that can be implemented by the actuators. Similarly, the control input constraints impose an upper bound on the required speed of convergence of $\rho_{s_m}(t), m \in \{1,\ldots,6\}$, as obtained by the exponentials $e^{-l_{s_m} t}$. Notice that (40)-(49) provide bounds on $\varepsilon_s, r_s$ and $\varepsilon_v, r_v$ that depend on the constants $\bar{B}_s$ and $\bar{B}_v$. Therefore, by invoking (27) and (35), we can select the control gains such $g_s$ and $g_v$ such that $v_{O,\text{des}}$ and $u_i$ are retained within certain bounds. Nevertheless, the constants $\bar{B}_s$ and $\bar{B}_v$ involve the parameters of the model, the external disturbances, and the performance specifications. Thus, an upper bound of the dynamic parameters of the system as well as the exogenous disturbances must be given in order to extract any relationship between the achieved performance and some potential input constraints, which are not taken into account in the current work.

### 4.2 High-Level Plan Generation

The second part of the proposed solution is the derivation of a high-level plan that satisfies the given MITL formula $\phi$ and can be generated using standard techniques from automata-based formal verification methodologies. Thanks to our proposed control law that allows the transition $\pi_j \xrightarrow{\mathcal{T}} \pi_{j'}$ for all $\pi_j \in \Pi$ with $\pi_{j'} \in \mathcal{D}(\pi_j)$ in a predefined time interval $\delta t_{j,j'}$, we can abstract the motion of the coupled object-agents system as a finite weighted transition system (WTS) (Baier et al., 2008)

$$\mathcal{T} = \{\Pi, \Pi_0, \xrightarrow{\mathcal{T}}, \mathcal{AP}, \mathcal{L}, \gamma\}, \tag{50}$$

where

- $\Pi$ is the set of states defined in Section 3.2,
- $\Pi_0 \subset \Pi$ is a set of initial states,
- $\xrightarrow{\mathcal{T}} \subseteq \Pi \times \Pi$ is a transition relation according to Definition 8.
- $\mathcal{AP}$ and $\mathcal{L}$ are the atomic propositions and the labeling function, respectively, as defined in Section 3.3, and
- $\gamma : (\xrightarrow{\mathcal{T}}) \to \mathbb{R}_{\geq 0}$ is a map that assigns to each transition its time duration, i.e., $\gamma(\pi_j \xrightarrow{\mathcal{T}} \pi_{j'}) = \delta t_{j,j'}$.

Therefore, by designing the switching protocol $U_{r_j}^{r_{j+1}}(t)$ from (35):

$$U_{r_j}^{r_{j+1}}(t) = -C_g G^*(q(t)) \rho_v^{-1}(t) r_v(\xi_v(t)) \varepsilon_v(\xi_v(t)), \quad \forall t \in [t_j, t_j + \delta t_{r_j, r_{j+1}}), \tag{51}$$

$j \in \mathbb{N}$, with (i) $t_1 = 0$, (ii) $t_{j+1} = t_j + \delta t_{r_j, r_{j+1}}$ and (iii) $r_j \in \{1, \ldots, R\}, \forall j \in \mathbb{N}$, we can define the *timed run* of the WTS as the infinite sequence $r = (\pi_{r_1}, t_1)(\pi_{r_2}, t_2)\ldots$, where $\pi_{r_1} \in \Pi_0$ with $\mathcal{A}(q(0)) \in \pi_{r_1}, \pi_{r_j} \in \Pi, r_j \in \{1, \ldots, R\}$ and $t_j$ are the corresponding time stamps such that $\mathcal{A}(q(t_j)) \in \pi_{r_j}, \forall j \in \mathbb{N}$. Every timed run $r$ generates the *timed word* $w(r) = (\mathcal{L}(\pi_{r_1}), t_1)(\mathcal{L}(\pi_{r_2}), t_2)\ldots$ over $\mathcal{AP}$ where $\mathcal{L}(\pi_{r_j}), j \in \mathbb{N}$, is the subset of the atomic propositions $\mathcal{AP}$ that are true when $\mathcal{A}(q(t_j)) \in \pi_{r_j}$.

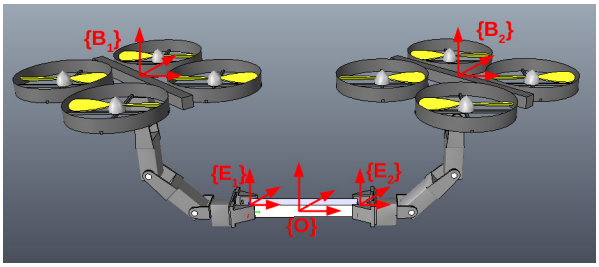


**Fig. 6** The aerial robots employed in the simulation rigidly grasping an object, with the frames $\{B_i\}, \{E_i\}, \{O\}, i \in \mathcal{N} = \{1, 2\}$.

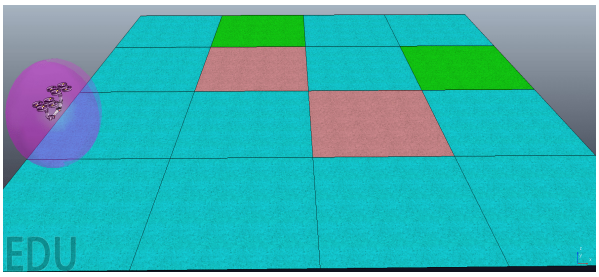


(a) Illustration of the initial workspace in the V-REP environment.

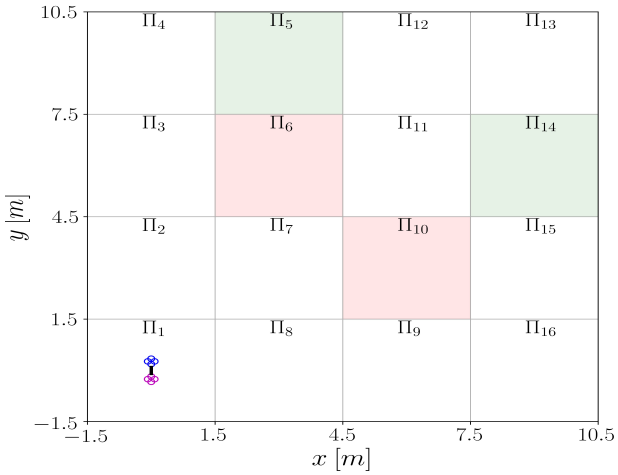


(b) Top-view of the initial workspace.

**Fig. 7** Illustration of the initial workspace and pose of the system object-agents in the V-REP environment (a) and in top view (b). The red cells imply obstacle regions whereas the green cells are the goal ones.

The given MITL formula $\phi$ is translated into a *Timed Büchi Automaton* $\mathcal{A}_\phi^t$ (Alur and Dill, 1994) and the product $\mathcal{A}_p = \mathcal{T} \otimes \mathcal{A}_\phi^t$ is built (Baier et al., 2008). The projection of the accepting runs of $\mathcal{A}_p$ onto $\mathcal{T}$ provides a *timed run* $r_\phi$ of $\mathcal{T}$ that satisfies $\phi$; $r_\phi$ has the form $r_\phi = (\pi_{r_1}, t_1)(\pi_{r_2}, t_2)\ldots$, i.e., an infinite[2] sequence of regions $\pi_{r_j}$ to be visited at specific time instants $t_j$ (i.e., $\mathcal{A}(q(t_j)) \in \pi_{r_j}$) with $t_1 = 0$ and $t_{j+1} = t_j + \delta t_{r_j, r_{j+1}}, r_j \in \{1, \ldots, R\}, \forall j \in \mathbb{N}$. More details on the technique are beyond the scope of this paper and the reader is referred to (Baier et al., 2008; Nikou et al., 2016; Alur and Dill, 1994).

The execution of $r_\phi = (\pi_{r_1}, t_1)(\pi_{r_2}, t_2)\ldots$ produces a trajectory $q(t), t \in \mathbb{R}_{\geq 0}$, with timed sequence $\beta_\phi = (q(t_1), t_1)(q(t_2), t_2)\ldots$, with $\mathcal{A}(q(t_j)) \in \pi_{r_j}, \forall j \in \mathbb{N}$. Following Definition 9, $\beta_\phi$ has the timed behavior $\sigma_{\beta_\phi} = (\sigma_1, t_1)(\sigma_2, t_2)\ldots$ with $\sigma_j \in \mathcal{L}(\pi_{r_j})$, for $\mathcal{A}(q(t_j)) \in \pi_{r_j}, \forall j \in \mathbb{N}$. Since all $\pi_{r_j}$ belong to $r_\phi, \forall j \in \mathbb{N}$, the latter implies that $\sigma_{\beta_\phi} \models \phi$ and

[2] It can be proven that if such a run exists, then there also exists a run that can be always represented as a finite prefix followed by infinite repetitions of a finite suffix (Baier et al., 2008).

therefore that $\beta_\phi$ satisfies $\phi$. The aforementioned discussion is summarized as follows:

**Theorem 3** *The execution of $r_\phi = (\pi_{r_1}, t_1)(\pi_{r_2}, t_2)\dots$ of $\mathcal{T}$ that satisfies $\phi$ guarantees a timed behavior $\sigma_{\beta_\phi}$ of the coupled object-agents system that yields the satisfaction of $\phi$ and provides, therefore, a solution to Problem 1.*

## 5 Simulation Results

The validity of the proposed framework is verified through a simulation study in the Virtual Robot Experimentation Platform (V-REP) (Rohmer et al., 2013). We consider a rectangular rigid body of dimensions $0.025 \times 0.2 \times 0.025$ m$^3$ representing the object that is rigidly grasped by two agents. Each agent $i \in \mathcal{N} = \{1,2\}$ consists of a quadrotor base $\{B_i\}$ and a robotic arm of two degrees of freedom $\alpha_{i_1}, \alpha_{i_2} \in [-\frac{\pi}{2}, \frac{\pi}{2}]$, as depicted in Fig. 6. The states of the agents are taken as $q_i = [p_{B_i}^T, \eta_{B_i}^T, \alpha_{i_1}, \alpha_{i_2}]^T \in \mathbb{R}^8$ and the control inputs as $\tau_i = [f_{B_i}^T, \mu_{B_i}^T, \tau_{\alpha_1}, \tau_{\alpha_2}]^T$, $i \in \{1,2\}$. We consider that the quadrotor is fully actuated, as mentioned in Section 3, and there exists an embedded algorithm that translates the generalized force $\lambda_{B_i} = [f_{B_i}^T, \mu_{B_i}^T]^T$ to the actual motor inputs.

The initial conditions of the system are taken such that $p_O(0) = [0,0,1.5]^T$ m, $\eta_O(0) = [0,0,0]^T$ r. The workspace is partitioned into $R = 16$ regions, with $\hat{L} = 0.75$ m and $l_0 = 0.5$ m. Fig. 7 illustrates the aforementioned setup at $t = 0$, from which it can be deduced that $\mathcal{A}(q(0)) \in \pi_1$. We further define the atomic propositions $\mathcal{AP} = \{$"green$_1$", "green$_2$", "red", "obs"$\}$, representing goal ("green$_1$", "green$_2$") and obstacle ('obs") regions with $\mathcal{L}(\pi_5) = \{$"green$_1$"$\}$, $\mathcal{L}(\pi_{14}) = \{$"green$_2$"$\}$, $\mathcal{L}(\pi_6) = \mathcal{L}(\pi_{10}) = \{$"obs"$\}$ and $\mathcal{L}(\pi_j) = \emptyset$, for the remaining regions.

We consider the MITL formula $\phi = (\Box_{[0,\infty)} \neg$"obs"$) \wedge \Diamond_{[0,60]}($"green$_1$"$\wedge \Diamond_{[0,24]}$"green$_2$"$)$, which describes the following behavior: the coupled system

(i) must always avoid the obstacle regions,

(ii) must visit the first green region in the first 60 seconds and after that visit the second green region in the next 24 seconds.

By following the procedure described in Section 4.2, we obtain the accepting timed run

$$\begin{aligned} r_\phi =& (\pi_{r_1}, t_1)(\pi_{r_2}, t_2)\dots \\ =& (\pi_1, 0)(\pi_2, 6)(\pi_3, 12)(\pi_4, 18)(\pi_5, 24)(\pi_{12}, 30)(\pi_{13}, 36) \\ & (\pi_{14}, 42)(\pi_{11}, 48)(\pi_{12}, 54)(\pi_5, 60). \end{aligned}$$

Regarding each transition $\pi_{r_j} \xrightarrow{\mathcal{T}} \pi_{r_{j+1}}$, $j \in \{1,\dots,10\}$, we choose $\delta t_{r_j, r_{j'}} = 6$ s, $p_{r_j, r_{j'}}(t)$ as in (21) and $\eta_{r_j, r_{j'}}(t) = [0, 0, \frac{\pi}{4}\sin(\frac{\pi}{3}(t - t_{r_j}))]^T$ [3], where $t_{r_j} = j\delta t_{r_j, r_{j'}} = 6j$ plays the role of $t_0$ for each transition. Regarding the performance function parameters, we choose $\rho_{p_k}^0 = \rho_{p_k}(t_{r_j}) = l_0 = 0.5$m, $l_{p_k} = 0.5$, $\rho_{p_k}^\infty = \lim_{t\to\infty} \rho_{p_k}(t) = 0.1$ m, $\forall k \in \{1,2,3\}$, $\rho_{\eta_\ell}^0 = \rho_{\eta_\ell}(t_{r_j}) = \frac{\pi}{2}$ r, $l_{\eta_\ell} = 0.5$, $\rho_{\eta_\ell}^\infty = \lim_{t\to\infty} \rho_{\eta_\ell}(t) = \frac{\pi}{12}$ r, $\forall \ell \in \{\phi, \theta, \psi\}$, $\rho_{v_m}^0 = \rho_{v_m}(t_{r_j}) = 2|e_{v_m}(t_{r_j})| + 0.5$, $l_{v_m} = 0.5$ and $\rho_{v_m}^\infty = \lim_{t\to\infty} \rho_{v_m}(t) = 0.1$, $m \in \{1,\dots,6\}$, $j \in \{1,\dots,10\}$. The two agents contribute equally to the task by choosing $c_1 = c_2 = 0.5$. Finally, the control gains are chosen as $g_s = 1$, $g_v = 10$.

The simulation results are depicted in Figs. 8-11. More specifically, Fig. 8 depicts the timed transitions of the coupled object-agents system, from which it can be deduced that $p_O(t) \in \mathcal{B}(p_{r_j, r_{j'}}, l_0)$ and therefore $p_s \in \pi_{r_j} \cup \pi_{r_{j'}}$, $\forall p_s \in \mathcal{S}_q$, $j \in \{1,\dots,10\}$. Moreover, Fig. 9 and 10 illustrate the errors $e_s(t)$ and $e_v(t)$ along with the performance functions $\rho_s(t), \rho_v(t)$, respectively, for all the transitions $\pi_{r_j} \to \pi_{r_{j'}}$, $j \in \{1,\dots,10\}$. Finally, the resulted control inputs $\tau_1, \tau_2$ for the two agents are shown in Fig. 11. The aforementioned simulation paradigm is illustrated in the accompanying video.

## 6 Conclusion and Future Work

We addressed the problem of defining timed abstractions for distributed cooperative manipulation of a single object by multiple robotic agents. We proposed a novel distributed control protocol for trajectory tracking of the object's center of mass with prescribed transient and steady performance, which allows us to abstract the motion of the coupled object-agents system as a weighted transition system. In that way, objectives regarding the overall system can be specified in terms of metric temporal logic formulas. Future efforts will be devoted towards compensating uncertainties in the object's geometrical characteristics, considering non-rigid grasps and generalizing the proposed framework for agents and objects scattered around the workspace.

## References

Adzkiya, D., De Schutter, B., and Abate, A. (2013). Finite abstractions of max-plus-linear systems. *IEEE Transactions on Automatic Control*, 58(12):3039–3053.

Aksaray, D., Vasile, C.-I., and Belta, C. (2016). Dynamic routing of energy-aware vehicles with temporal logic constraints. *Proceedings of the IEEE International Conference on Robotics and Automation (ICRA)*, pages 3141–3146.

Alur, R. and Dill, D. L. (1994). A theory of timed automata. *Theoretical computer science*, 126(2):183–235.

Alur, R., Feder, T., and Henzinger, T. A. (1996). The benefits of relaxing punctuality. *Journal of the ACM (JACM)*, 43(1):116–146.

[3] Note that the nature of the quadrotors makes the whole system underactuated and values $\phi_{r_j, r_{j'}}(t), \theta_{r_j, r_{j'}}(t) \neq 0$ are not possible to be achieved without interfering with $p_O(t)$.

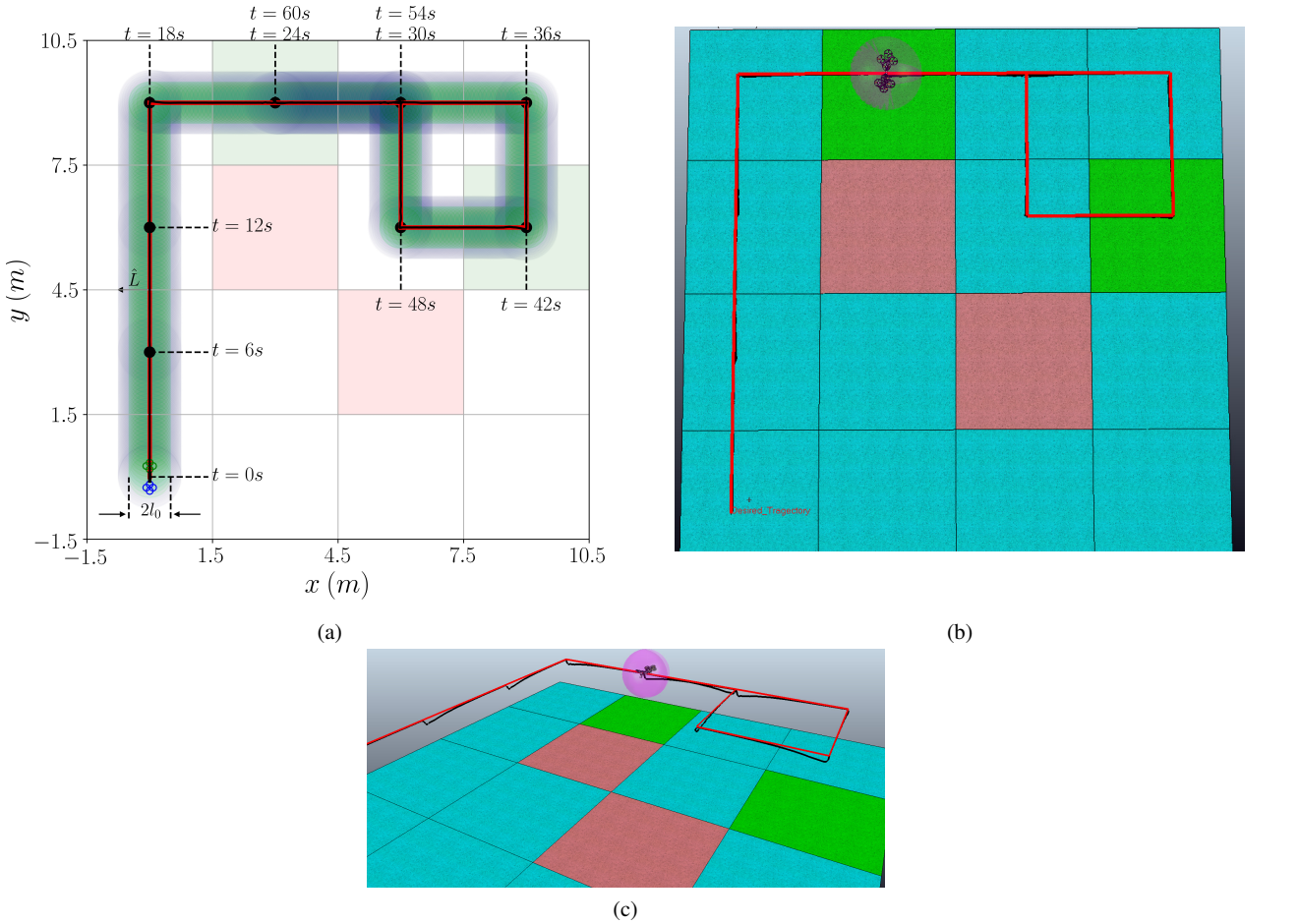


**Fig. 8** (a): The overall desired object trajectory (with red), the actual object trajectory (with black), the domain specified by $\mathcal{B}(p_{r_j,r_{j'}}(t), l_0), \forall j \in \{1,\ldots,10\}$ (with green), and the domain specified by $\mathcal{B}(p_o(t), \hat{L})$ (with blue), for $t \in [0,60]$ s. (b), (c): Illustration of the system at the final region at $t = 60$s in the V-REP environment along with the ball $\mathcal{B}(p_o(60), \hat{L})$. Since $p_o \in \mathcal{B}(p_{r_j,r_{j'}}(t), l_0)$, the desired timed run is successfully executed.


Baier, C., Katoen, J.-P., et al. (2008). *Principles of model checking*. MIT press Cambridge.

Bechlioulis, C. P. and Rovithakis, G. A. (2014). A low-complexity global approximation-free control scheme with prescribed performance for unknown pure feedback systems. *Automatica*, 50(4):1217–1226.

Belta, C. and Habets, L. C. (2006). Controlling a class of nonlinear systems on rectangles. *IEEE Transactions on Automatic Control*, 51(11):1749–1759.

Belta, C. and Kumar, V. (2004). Abstraction and control for groups of robots. *IEEE Transactions on robotics*, 20(5):865–875.

Boskos, D. and Dimarogonas, D. V. (2015). Decentralized abstractions for feedback interconnected multi-agent systems. *Proceedings of the IEEE Conference on Decision and Control (CDC)*, pages 282–287.

Caccavale, F., Chiacchio, P., Marino, A., and Villani, L. (2008). Six-dof impedance control of dual-arm cooperative manipulators. *IEEE/ASME Transactions On Mechatronics*, 13(5):576–586.

Chaimowicz, L., Campos, M. F. M., and Kumar, V. (2003). Hybrid systems modeling of cooperative robots. *Proceedings of the IEEE International Conference on Robotics and Automation (ICRA)*, 3:4086–4091.

Chen, Y., Ding, X. C., Stefanescu, A., and Belta, C. (2012). Formal approach to the deployment of distributed robotic teams. *IEEE Transactions on Robotics*, 28(1):158–171.

Cheng, P., Fink, J., and Kumar, V. (2009). Abstractions and algorithms for cooperative multiple robot planar manipulation. *Robotics: Science and Systems IV*, page 143.

Diaz-Mercado, Y., Jones, A., Belta, C., and Egerstedt, M. (2015). Correct-by-construction control synthesis for multi-robot mixing. *Proceedings of the IEEE Conference on Decision and Control (CDC)*, pages 221–226.

Erhart, S. and Hirche, S. (2013). Adaptive force/velocity control for multi-robot cooperative manipulation under uncertain kinematic parameters. *Proceedings of the IEEE/RSJ International Conference on Intelligent Robots*

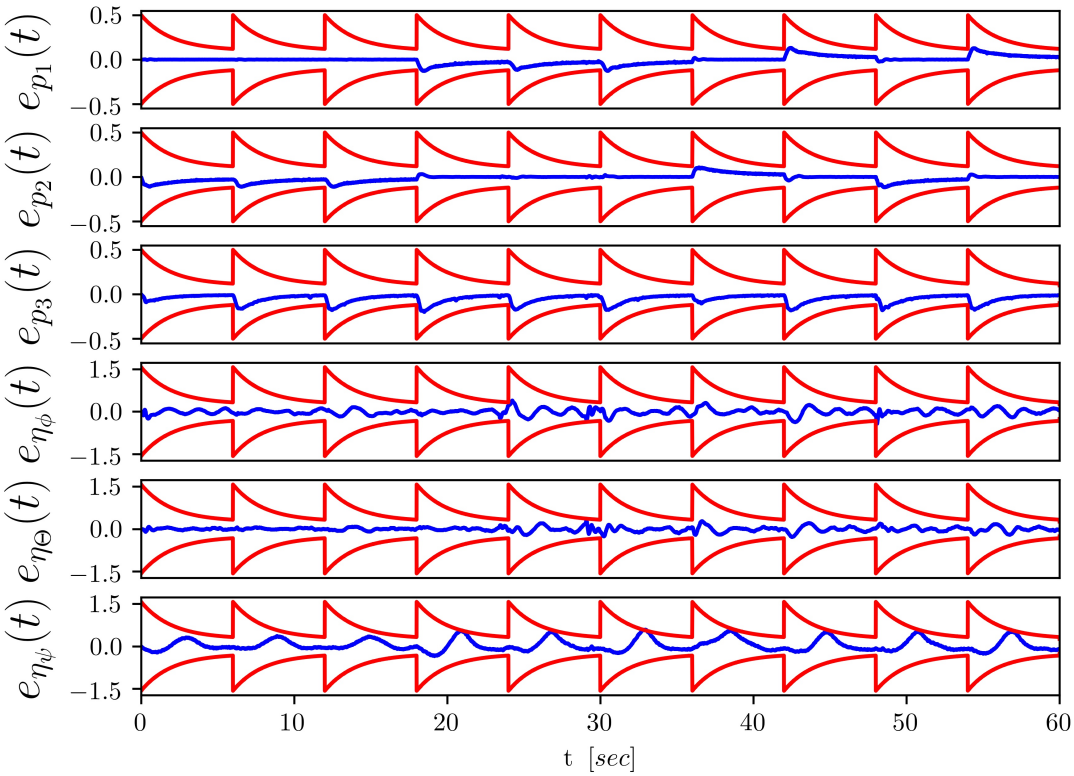


**Fig. 9** The pose errors $e_s(t)$ (with blue) along with the performance functions $\rho_s(t)$ (with red) (in $m, m, m, r, r, r$, respectively).

*and Systems (IROS)*, pages 307–314.

Filippidis, I. and Murray, R. M. (2016). Symbolic construction of gr (1) contracts for systems with full information. *Proceedings of the American Control Conference (ACC)*, pages 782–789.

Franchi, A., Petitti, A., and Rizzo, A. (2014). Distributed estimation of the inertial parameters of an unknown load via multi-robot manipulation. In *IEEE Conference on Decision and Control (CDC)*, pages 6111–6116. IEEE.

Franchi, A., Petitti, A., and Rizzo, A. (2015). Decentralized parameter estimation and observation for cooperative mobile manipulation of an unknown load using noisy measurements. In *IEEE International Conference on Robotics and Automation (ICRA)*, pages 5517–5522. IEEE.

Guo, M., Tumova, J., and Dimarogonas, D. V. (2014). Cooperative decentralized multi-agent control under local ltl tasks and connectivity constraints. *Proceedings of the IEEE International Conference on Decision and Control*, pages 75–80.

He, K., Lahijanian, M., Kavraki, L. E., and Vardi, M. Y. (2015). Towards manipulation planning with temporal logic specifications. *Proceedings of the IEEE International Conference on Robotics and Automation (ICRA)*, pages 346–352.

Heck, D., Kostic, D., Denasi, A., and Nijmeijer, H. (2013). Internal and external force-based impedance control for cooperative manipulation. *Proceedings of the IEEE European Control Conference (ECC)*, pages 2299–2304.

Karaman, S. and Frazzoli, E. (2011). Linear temporal logic vehicle routing with applications to multi-uav mission planning. *International Journal of Robust and Nonlinear Control*, 21(12):1372–1395.

Kloetzer, M. and Belta, C. (2008). A fully automated framework for control of linear systems from temporal logic specifications. *IEEE Transactions on Automatic Control*, 53(1):287–297.

Lionis, G. and Kyriakopoulos, K. J. (2005). Centralized motion planning for a group of micro agents manipulating a rigid object. *Proceedings of the IEEE International Symposium on Intelligent Control, Mediterrean Conference on Control and Automation*, pages 662–667.

Lippiello, V. and Ruggiero, F. (2012). Cartesian impedance control of a uav with a robotic arm. *IFAC Proceedings Volumes*, 45(22):704 – 709.

Liu, Y.-H. and Arimoto, S. (1998). Decentralized adaptive and nonadaptive position/force controllers for redundant

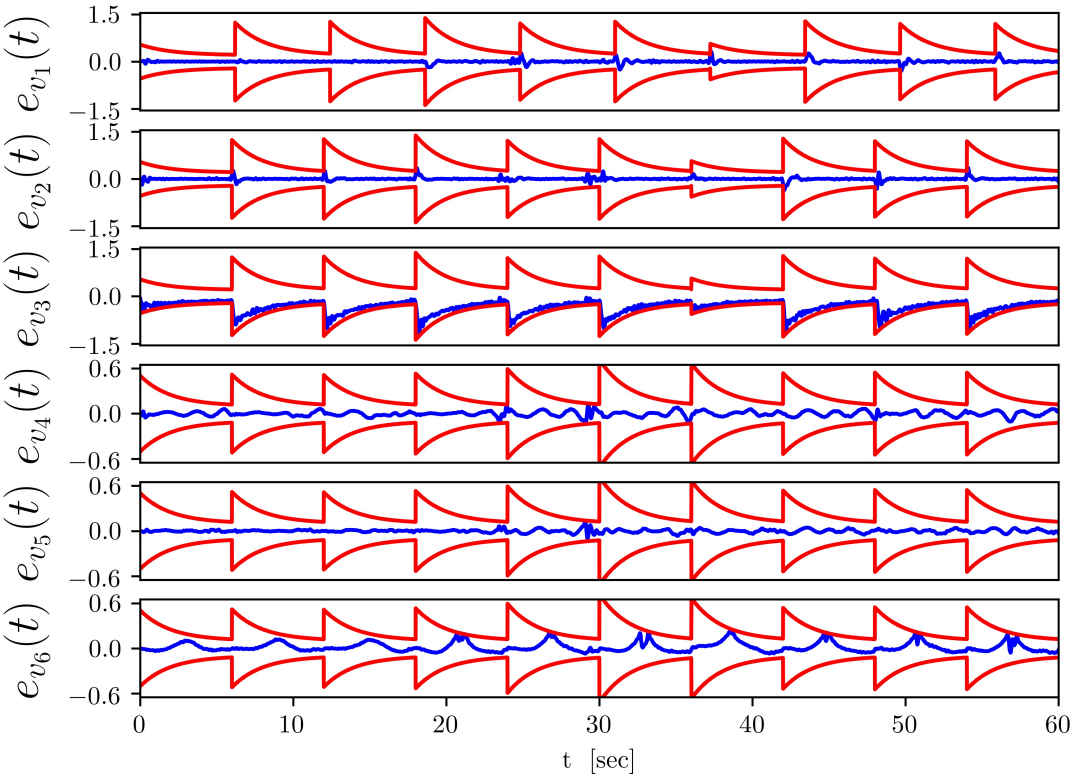


**Fig. 10** The velocity errors $e_v(t)$ (with blue) along with the performance functions $\rho_v(t)$ (with red) (in $m/s, m/s, m/s, r/s, r/s, r/s$, respectively).

manipulators in cooperations. *The International Journal of Robotics Research*, 17(3):232–247.

Markdahl, J., Karayiannidis, Y., and Hu, X. (2012). Cooperative object path following control by means of mobile manipulators: a switched systems approach. *IFAC Proceedings Volumes*, 45(22):773–778.

Michael, N., Fink, J., and Kumar, V. (2011). Cooperative manipulation and transportation with aerial robots. *Autonomous Robots*, 30(1):73–86.

Muthusamy, R. and Kyrki, V. (2014). Decentralized approaches for cooperative grasp planning. *Proceedings of the International Conference on Control Automation Robotics & Vision (ICARCV),*, pages 693–698.

Nikou, A., Tumova, J., and Dimarogonas, D. V. (2016). Cooperative task planning of multi-agent systems under timed temporal specifications. *Proceedings of the IEEE American Control Conference (ACC)*, pages 7104–7109.

Ouaknine, J. and Worrell, J. (2005). On the decidability of metric temporal logic. *Annual IEEE Symposium on Logic in Computer Science (LICS'05)*, pages 188–197.

Palunko, I., Donner, P., Buss, M., and Hirche, S. (2014). Cooperative suspended object manipulation using reinforcement learning and energy-based control. In *IEEE/RSJ International Conference on Intelligent Robots and Systems (IROS 2014)*, pages 885–891. IEEE.

Parra-Vega, V., Sanchez, A., Izaguirre, C., Garcia, O., and Ruiz-Sanchez, F. (2013). Toward aerial grasping and manipulation with multiple uavs. *Journal of Intelligent & Robotic Systems*, 70(1-4):575–593.

Petitti, A., Franchi, A., Di Paola, D., and Rizzo, A. (2016). Decentralized motion control for cooperative manipulation with a team of networked mobile manipulators. *Proceedings of the IEEE International Conference on Robotics and Automation (ICRA)*, pages 441–446.

Reissig, G. (2011). Computing abstractions of nonlinear systems. *IEEE Transactions on Automatic Control*, 56(11):2583–2598.

Rohmer, E., Singh, S. P., and Freese, M. (2013). V-rep: a versatile and scalable robot simulation framework. *Proceedings of The International Conference on Intelligent Robots and Systems (IROS)*.

Rungger, M., Weber, A., and Reissig, G. (2015). State space grids for low complexity abstractions. *Proceedings of the IEEE Conference on Decision and Control (CDC)*, pages 6139–6146.

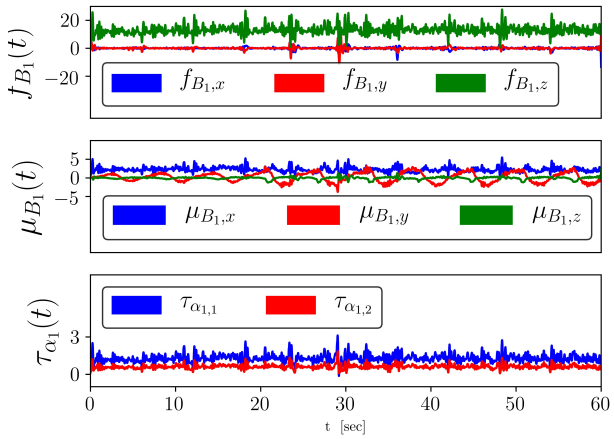


(a) The resulting control inputs $\tau_1(t)$ (in $N$, $Nm$, and $Nm$, respectively).

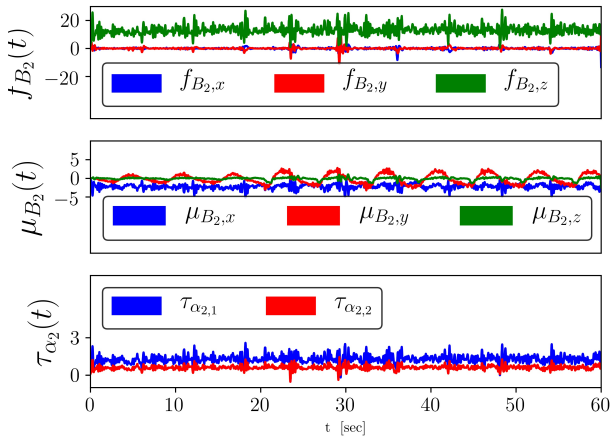


(b) The resulting control inputs $\tau_2(t)$ (in $N$, $Nm$, and $Nm$, respectively)..

**Fig. 11** The resulting control inputs $\tau_i = [f_{B_i}^T, \mu_{B_i}^T, \tau_{\alpha_{i,1}}, \tau_{\alpha_{i,2}}]$ for $i = 1$ (a) and $i = 2$ (b).


Siciliano, B. and Khatib, O. (2008). *Springer handbook of robotics*. Springer Science & Business Media.

Sontag, E. D. (2013). *Mathematical control theory: deterministic finite dimensional systems*, volume 6. Springer Science & Business Media.

Souza, D. and Prabhakar, P. (2007). On the expressiveness of mtl in the pointwise and continuous semantics. *International Journal on Software Tools for Technology Transfer*, 9(1):1–4.

Stroupe, A., Huntsberger, T., Okon, A., and Aghazarian, H. (2005). Precision manipulation with cooperative robots. *Multi-Robot Systems. From Swarms to Intelligent Automata Volume III*, pages 235–248.

Sugar, T. G. and Kumar, V. (2002). Control of cooperating mobile manipulators. *IEEE Transactions on robotics and automation*, 18(1):94–103.

Szewczyk, J., Plumet, F., and Bidaud, P. (2002). Planning and controlling cooperating robots through distributed impedance. *Journal of Robotic Systems*, 19(6):283–297.

Tanner, H. G., Loizou, S. G., and Kyriakopoulos, K. J. (2003). Nonholonomic navigation and control of cooperating mobile manipulators. *IEEE Transactions on Robotics and Automation*, 19(1):53–64.

Tiwari, A. (2008). Abstractions for hybrid systems. *Formal Methods in System Design*, 32(1):57–83.

Tsiamis, A., Tumova, J., Bechlioulis, C. P., Karras, G. C., Dimarogonas, D. V., and Kyriakopoulos, K. J. (2015a). Decentralized leader-follower control under high level goals without explicit communication. *Proceedings of the IEEE/RSJ International Conference on Intelligent Robots and Systems (IROS)*, pages 5790–5795.

Tsiamis, A., Verginis, C. K., Bechlioulis, C. P., and Kyriakopoulos, K. J. (2015b). Cooperative manipulation exploiting only implicit communication. *Proceedings of the IEEE/RSJ International Conference on Intelligent Robots and Systems (IROS)*, pages 864–869.

Verginis, C. K. and Dimarogonas, D. V. (2016). Distributed cooperative manipulation under timed temporal specifications. *American Control Conference (ACC)*.

Wang, Z. and Schwager, M. (2016). Multi-robot manipulation without communication. *Distributed Autonomous Robotic Systems*, pages 135–149.

Yamashita, A., Arai, T., Ota, J., and Asama, H. (2003). Motion planning of multiple mobile robots for cooperative manipulation and transportation. *IEEE Transactions on Robotics and Automation*, 19(2):223–237.

Zamani, M., Mazo, M., and Abate, A. (2014). Finite abstractions of networked control systems. *Proceedings of the IEEE Conference on Decision and Control*, pages 95–100.

Zhang, Z. and Cowlagi, R. V. (2016). Motion-planning with global temporal logic specifications for multiple nonholonomic robotic vehicles. *Proceedings of the American Control Conference (ACC)*, pages 7098–7103.